ORGANOMETALLICS

Article

Cite This: Organometallics XXXX, XXX, XXX-XXX pubs.acs.org/Organometallics

Rh and Ir β-Diiminate Complexes of Boranes, Silanes, Germanes, and Stannanes

Nan Zhang,[†] Rebecca S. Sherbo,[†,∥] Gurmeet Singh Bindra,[†,⊥] Di Zhu,[†,‡] and Peter H. M. Budzelaar*[,†,§]

[†]Department of Chemistry, University of Manitoba, 144 Dysart Road, Winnipeg, Manitoba R3T 2N2, Canada

[‡]State Key Laboratory of Heavy Oil Processing, College of Science, China University of Petroleum, Beijing 102249, People's Republic of China

[§]Department of Chemical Sciences, Federico II University of Naples, Via Cintia, Complesso di Monte S. Angelo, 80126 Napoli, Italy

Supporting Information

ABSTRACT: Reported here are several new adducts of the type (^{R}BDI)M(HE)$_2$ where ^{R}BDI is the β-diiminate ligand [2,6-R$_2$C$_6$H$_3$N═CMe]$_2$CH (R = Me, Et, MeO; M = Rh, Ir; HE = HSiEt$_3$, HGeEt$_3$, HSn^{n}Bu$_3$, HBPin). DFT calculations are used to analyze the bonding in these and related Cp* complexes, in particular with respect to the degree of oxidative addition (OA) of the H−E bonds: this increases in the order H$_2$ < HBPin < HSiEt$_3$ ≈ HGeEt$_3$ ≈ HSn^{n}Bu$_3$, it proceeds further for Ir than for Rh, and Cp* promotes OA to a larger degree in comparison to the BDI ligand. The *first* metal−HE dissociation energy is rather sensitive to steric effects and increases in the order CH$_4$ ≪ H$_2$ ≈ HBPin ≈ HSiMe$_3$ ≈ HGeMe$_3$ < HSnMe$_3$, with Ir uniformly binding HE more strongly than Rh by about 10 kcal/mol. M−HE dissociation is the first step of the intramolecular ligand functionalization first reported for (^{Me}BDI)Rh(HSiEt$_3$)$_2$. Such functionalization was not observed for any of the new complexes reported here. On the basis of the idea that stannane dissociation might be prohibitive, we obtained evidence that it is possible to effect such functionalization via generation of a stannane within the coordination sphere of the metal: treatment of (^{Me}BDI)Rh(COE)(N$_2$) with SnMe$_4$ and H$_2$ produced a mixture of (^{Me}BDI)Rh(HSnMe$_3$)$_2$ and its functionalized derivative (^{Me}BDI∧SnHMe$_2$)Rh(HSnMe$_3$) via Sn−C cleavage.

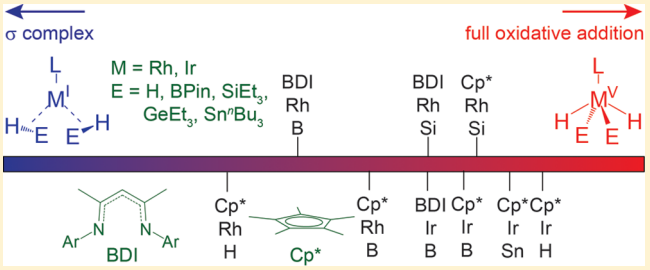

INTRODUCTION

Oxidative addition of C−H and X−H bonds ranks among the most important elementary steps in organometallic catalysis. The reaction requires a coordinatively unsaturated metal center in a low oxidation state. Since coordinative unsaturation is often associated with high reactivity, well-characterized examples of X−H addition often involve bulky ligands that shield the metal center from various unwanted side reactions.

Cp*Rh and Cp*Ir fragments (often generated in situ) are very effective in activating even unreactive C−H bonds.[1−4] The Cp* ligand stabilizes high oxidation states, and examples of formally M^{V} complexes (Chart 1, structural type B) such as Cp*IrH$_4$[5] and Cp*RhH$_2$(SiEt$_3$)$_2$[6] have been reported. There is always some ambiguity about the "actual" oxidation state[7] of the metal atom in such complexes, since they can also be viewed as M^{I} σ complexes (Chart 1, structural type A) or perhaps some intermediate structure. Presumably the locations of the hydrogen atoms could distinguish between these alternatives, but the problems associated with accurately locating H atom positions near heavy atoms in X-ray structure determinations mean that uncertainty remains.

Because of this ambiguity, bonding in Cp*M(HE)$_2$ complexes (M = Rh, Ir; HE = silane, germane, stannane, borane) has been studied by several groups, using both experimental (NMR, X-ray and neutron diffraction, IR) and computational (DFT) methods. As early as 1984, Fernandez et al. reported the synthesis of Cp*Rh(HSiEt$_3$)$_2$ and its full characterization (including neutron diffraction),[6] leading to identification as a dihydride (Rh^{V}) species. Values for J_{RhH} (37 Hz) and J_{SiH} (8 Hz) were reported. The structure of the isomorphous Ir analogue was reported shortly thereafter[8−10] (no J_{SiH} value reported). A few years later Duckett and co-workers generated CpRh(HSiEt$_3$)$_2$ and concluded, in part on

Chart 1. Extreme Interpretations of Cp*M(HE)$_2$ and (BDI)M(HE)$_2$ structures

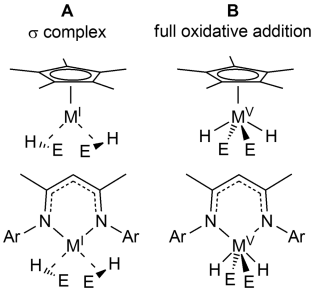

Received: June 20, 2017

DOI: 10.1021/acs.organomet.7b00469
Organometallics XXXX, XXX, XXX−XXX

the basis of a sizable J_{RhH} value of 38 Hz and a small J_{SiH} value of 7 Hz, that a dihydride structure was more plausible than the σ-silane alternative.[11] They then prepared several CpRhH-$(SiR_3)_3$ complexes and described these as containing Rh^V but also having some η^2-silane character, on the basis of substantially larger Si−H coupling constants (>20 Hz).[12] This J_{SiH} criterion (20−70 Hz indicating residual interactions[13])) has been cited frequently, but recently Scherer et al. argued that interpretation of these coupling constants may not always be straightforward since near the oxidative-addition range of the reaction trajectory the observed J value is the sum of a negative $^1J_{SiH}$ and a positive $^2J_{SiH}$ contribution that nearly cancel.[14] Vyboishchikov and Nikonov performed a careful DFT analysis of the above CpRh bis(silyl) and tris(silyl) complexes[15] and concluded that there are weak residual Si−H interactions, implying that a description as Rh^V is not completely correct (though presumably better than Rh^I or Rh^{III} alternatives). They also emphasized that the energy surface for stretching or compressing the Si−H "bonds" is extremely flat so that a particular observed geometry does not tell the whole story. In an experimental study on related Cp*Rh(PMe_3)(silane)$^+$ complexes, Taw et al. noted formation of σ-silane derivatives[16] in cases where the analogous Ir complex tends toward full oxidative addition,[17] and this seems to be a rather general feature.

In any case, it seems to be generally accepted that Cp*M$(HSiR_3)_2$/CpM$(HSiR_3)_2$ complexes are best regarded as having M^V (with some residual Si−H interaction) but the situation is somewhat less clear for analogous complexes of boranes, germanes, and stannanes. Cook et al. have reported the formation of Cp*Rh(HBPin)$(HSiEt_3)$ and concluded on the basis of an X-ray structure and DFT studies[18] that the bonding is more ambiguous than in Cp*Rh$(HSiEt_3)_2$, featuring one relatively short B−H contact (X-ray, 1.745 Å; DFT, 1.970 Å). The somewhat broadened hydride signal (12 Hz, narrowing to 8 Hz on ^{11}B decoupling; J_{RhH} = 42 Hz) was also taken as evidence for some degree of B−H interaction. Nevertheless, the structure is probably closer to an Rh^V(H)(boryl) complex than to a Rh^{III}(σ-borane) species. Soon after, the group of Hartwig also reported the synthesis and characterization of Cp*Rh-$(HBPin)_2$ and Cp*RhH$(BPin)_3$ and concluded that these have some σ-borane character, on the basis of X-ray structures and of broadened hydride signals (40 and 32 Hz)[19] (in contrast, the hydride signal of Cp*Ir$(HBPin)_2$ is sharp[1]). DFT studies confirmed the presence of short B−H contacts but also revealed that these contacts can be stretched or compressed with very low energetic cost: the calculated free energy barrier for switching B−H contacts is only 0.8 kcal/mol.

Very few Cp*M stannane complexes have been reported. The X-ray structure of Cp*IrH_3SnPh_3 shows a four-legged piano-stool geometry (shortest Sn−H contact 2.42 Å);[20] the ^{1}H NMR spectrum showed separate trans and cis hydride signals at low temperature, which coalesced on warming to a single resonance with average J_{SnH} value of 28 Hz (Cp*IrH_3SnMe_3 behaved similarly). Both the reported piano-stool geometry and the relatively small J_{SnH} value indicate a mostly Ir^V structure; for comparison, $(C_5H_4Me)Mn(CO)_2(HSnPh_3)$ has been assigned a σ-stannane structure on the basis of the short Sn−H distance of 2.16 Å (X-ray) and a large J_{SnH} value of 270 Hz.[21]

Recently, the group of Crimmin reported on the synthesis, characterization, and DFT studies of Cp*Rh$(HSiEt_3)$(HZ) complexes where Z = (^{Me}BDI)AlH, (^{Me}BDI)Zn, (^{Me}BDI)Mg.[22] They concluded that the dominant description is that of an oxidative-addition product, but with significant residual H−Z interactions. For the more electropositive Zn and Mg fragments, the negative charge on Rh becomes significant and a dihydridorhodate limiting structure contributes.

The β-diiminate (BDI) ligand (Chart 2) has proven to be very effective in stabilizing low-coordinate metal environments

Chart 2. The Basic ^{R}BDI Ligand and Other Specific Ligand Variations Mentioned in the Text

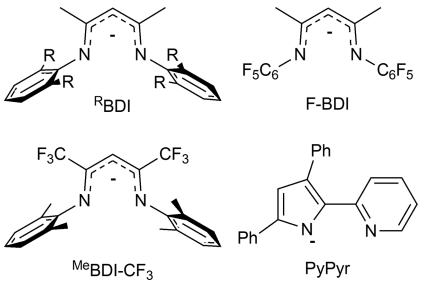

and in allowing isolation and characterization of species that with other ligands would be reactive intermediates.[23] We[24] and others[25] have noted that there are certain parallels between the chemistry of Cp* and BDI ligands, in particular in combination with the group 9 metals Rh and Ir. In a mini-review,[26] we concluded that there are significant similarities but that Cp* is decidedly a more strongly donating ligand.

We recently reported the formation of (^{Me}BDI)Rh$(HSiEt_3)_2$ (**1**) and its further rearrangement to the complex (^{Me}BDI∧SiHEt$_2$)Rh$(HSiEt_3)$ (**1′**) involving Si−C cleavage and ligand functionalization (Scheme 1).[27] Extension to an

Scheme 1. Intramolecular Ligand Functionalization of (^{Me}BDI)Rh$(HSiEt_3)_2$ (1) to 1′

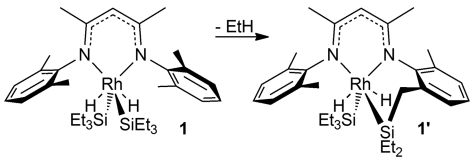

intermolecular, catalytic version would be of obvious interest. Transition-metal-catalyzed silylation and subsequent functionalization of even unactivated C−H bonds has become a useful tool in organic transformations, mainly due to work by the group of Hartwig, using Rh and Ir catalysis.[28,29] The field is dominated by arene C−H activation, but a recent report demonstrates that also unactivated C(sp^3)−H bonds can be selectively functionalized.[30]

The functionalization of **1** was proposed to start with dissociation of one HE (silane/germane) unit from the complex, followed by a cascade of bond-breaking and -forming steps. In view of this, the ease of HE dissociation from (BDI)Rh$(HE)_2$ is expected to be important. In the present paper, we report several new (^{R}BDI)M$(HE)_2$ complexes (HE = $HSiEt_3$, $HGeEt_3$, HSn^nBu_3, HBPin). Structure and bonding in Cp*M$(HE)_2$ and (^{R}BDI)M$(HE)_2$ are analyzed and compared on the basis of crystal structures and DFT calculations, focusing on the position of various LM$(HE)_2$ complexes between the extremes of pure σ complex and full oxidative addition (Chart 1). Trends in HE dissociation energies are explored as a function of metal, ligand, and substrate variation. While no

DOI: 10.1021/acs.organomet.7b00469
Organometallics XXXX, XXX, XXX−XXX

rearrangement analogous to that in Scheme 1 was observed starting with isolated stannane complexes, we report evidence that a stannane-functionalized BDI ligand can be generated by treating (^{Me}BDI)Rh(COE)(N_2) with $SnMe_4$ and H_2, presumably via formation of $HSnMe_3$ within the coordination sphere of the metal.

RESULTS AND DISCUSSION

New Complexes. In the present work we systematically examine the complexation of (^{R}BDI)M fragments (R = Me, Et, MeO; M = Rh, Ir) with HE compounds $HSiEt_3$, $HGeEt_3$, HSn^nBu_3, and HBPin. The complexes studied are given in Chart 3. The synthesis and X-ray structures of **1** and **1′** have

Chart 3. (^{R}BDI)M(HE)$_2$ Complexes Studied Experimentally

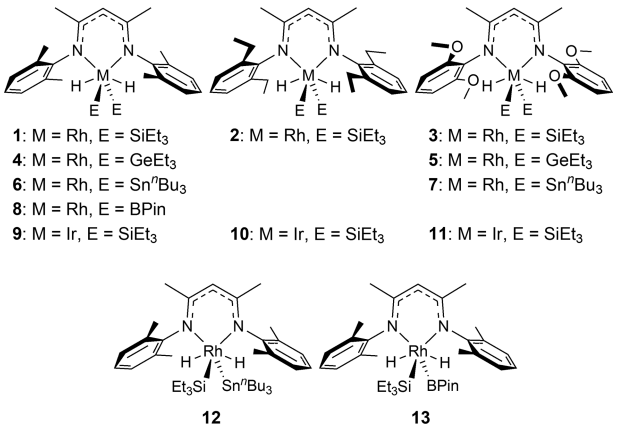

been reported in earlier work.[27] Several related complexes were mentioned in that communication, including **2**–**5**, but these were only characterized by ^{1}H NMR spectroscopy. Since then, Meier et al.[31] reported the formation of (F-BDI)Rh($HSiMe_3$)$_2$ from (F-BDI)Rh(CO)(NCMe) and excess $HSiMe_3$; the complex was not structurally characterized, but DFT studies produced a structure roughly similar to complex **1**. Relevant in this context is also the structure of (^{iPr}BDI)IrH_4 reported in 2004.[25]

Complexes **3**, **5**, and **7** were prepared by generating (^{MeO}BDI)Rh(COE) in situ and reacting it with a stoichiometric amount (**5**) or excess (**3**, **7**) of HE. Attempts to prepare **6** in a similar manner always resulted in mixtures of the desired product, the free ligand (^{Me}BDI)H, and unidentified impurities. For the synthesis of **8**, which is not very stable, it proved beneficial to use isolated (^{Me}BDI)Rh(COE). The three Ir complexes **9**–**11** were obtained by reacting $[Ir(COE)_2Cl]_2$ first with an excess of $HSiEt_3$ and then with 1 equiv of (^{R}BDI)Li. Efforts to prepare (^{Et}BDI)Rh(HSn^nBu_3)$_2$ failed, as did attempted syntheses of HBPin complexes other than **8** or Ir complexes with HE other than $HSiEt_3$. In all of these reactions we observed the formation of (^{R}BDI)H but could not identify any organometallic products. Two examples of mixed HE/HE′ complexes were isolated: complex **12** was obtained by sequentially adding 2.2 equiv of $HSiEt_3$ and 1 equiv of HSn^nBu_3 to a solution of (^{Me}BDI)Rh(COE), while complex **13** was easily obtained via comproportionation of **1** and **8**. All compounds are air-sensitive and most decompose slowly in solution (**8** within 1 day); they are stable in the solid state, under inert atmosphere, at −35 °C. None of the new complexes show clean rearrangement to a ligand-functionalized complex analogous to the transformation of **1** to **1′**. The dominant decomposition product is in most cases free (^{R}BDI)H; for Ir complexes, a black precipitate of metallic Ir was frequently observed. We have not been able to identify any Rh- or Ir-containing decomposition products, although for **8** high-field triplets (∼−20 ppm in ^{1}H NMR) are highly suggestive of formation of dinuclear hydrides similar to complexes reported by the group of Tilley.[32]

NMR Spectroscopic Characterization. Bis(HE) complexes **1**-**11** show effective C_{2v} symmetry in solution, with two equivalent E groups and two equivalent hydrides. The mixed complexes **12** and **13** appear C_s symmetric, with a single hydride (2H) signal but inequivalent "top" and "bottom" sides of the BDI ligand. The most characteristic and informative signals are the hydride resonances, which are found between −13.6 and −15.6 ppm for Rh or around −16.5 ppm for Ir. All Rh complexes show well-defined Rh−H coupling constants with magnitudes that seem to depend mostly on the nature of E, decreasing in the order BPin (∼25 Hz) > $SiEt_3$ (∼21 Hz) > $GeEt_3$ (15 Hz) > Sn^nBu_3 (∼12 Hz); these are a bit smaller than those observed for the corresponding Cp* complexes (vide supra).

The observation of clear Rh couplings on sharp (except for **8** and **12**) hydride resonances rules out dissociation of HE on the NMR time scale, although the synthesis of **13** via comproportionation proves that HE dissociation does happen at a longer time scale. This is similar to the behavior of (PyPyr)Rh($HSiRPh_2$)$_2$ (R = Ph, ^{t}Bu), where silane dissociation is slow on the NMR time scale and rate-limiting for silane exchange with $HSiEt_3$.[32]

For Rh-silane complexes **2**, **3**, and **12**, J_{SiH} values could be determined from ^{29}Si satellites as being 9, 10, and 8 Hz, respectively; for Ir silane complexes **9**–**11** no ^{29}Si satellites could be resolved, indicating $|J_{SiH}| < 3$ Hz.[33] These small J_{SiH} values firmly place the silane complexes in the "mostly classical" category. However, in view of work by Scherer et al.[14] the smaller J_{SiH} observed for Ir than for Rh complexes does not necessarily mean that oxidative addition has progressed further for Ir than for Rh.

HBPin complexes **8** and **12** show some broadening of the hydride signals (33 and 14 Hz, respectively) likely due to residual coupling to B, which suggests a degree of direct B−H interaction (cf. 40 Hz for Cp*Rh($HBPin$)$_2$[19]). ^{119}Sn/^{117}Sn satellites were observed for the hydride signals of **6**, 7, and **12** (22, 23, and 24 Hz, respectively). These couplings are much smaller than direct $^1J_{SnH}$ couplings,[34] indicating structures close to the oxidative-addition extreme.

X-ray Structure Determinations. The structures of complexes **2**, **3**, **5**, and **7**–**13** have been determined by X-ray diffraction. In all cases, hydrogens were located and refined at expected hydride positions but the usual caveat about H atoms near heavy atoms applies. Stick drawings of representative examples (**5**, **7**, **10**, and **13**) emphasizing the metal coordination environment are shown in Figure 1; thermal ellipsoid plots for all structures, showing the adopted numbering schemes and important bond lengths and angles, are included in the Supporting Information.

The molecular shapes can be described as a roughly tetrahedral N_2E_2M environment with hydrides each capping a NE_2 face, similar to the case for Rh and Ir complexes (PyPyr)M($HSiRPh_2$)$_2$.[32] An alternative, which we prefer because it facilitates comparison with Cp* complexes, is to look at the BDI ligand as occupying a single position at the bisector of the NMN angle: this leads to a description as a four-

DOI: 10.1021/acs.organomet.7b00469
Organometallics XXXX, XXX, XXX−XXX

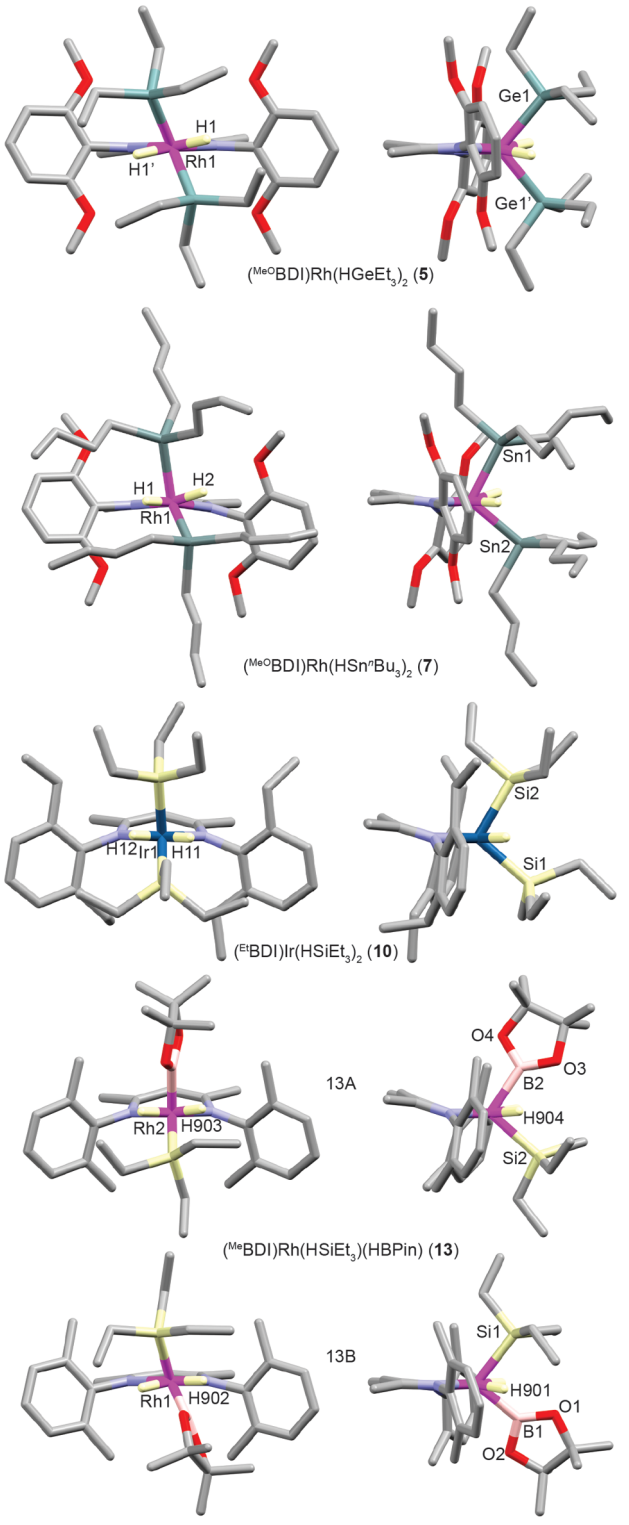

Figure 1. X-ray structures of **5**, **7**, **10**, and **13** (for full labeling schemes see the Supporting Information). All hydrogens except hydrides are omitted for clarity. For each structure, two projections are shown that emphasize T and R deformations: the left view looks up the piano stool (N–N vector horizontal), and the right view is along the N–N vector. **13A,B** are the two independent molecules in the unit cell of **13**; for **5**, only one of three independent molecules is shown.

legged piano stool. In either picture, the idealized geometry has the C_{2v} symmetry suggested by the solution NMR data. The structures actually observed exhibit two types of significant deformations away from this idealized geometry. The first one ("T") has the axis of the piano stool tilted out of the NMN plane, so that one E group ends up in a roughly apical position (relative to the BDI plane) while the second E group occupies an equatorial position (Figure 2). The resulting structure has

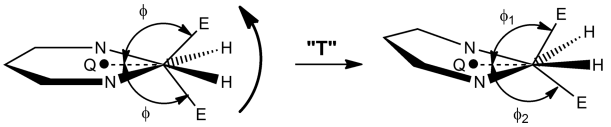

Figure 2. Schematic representation of T type deformation from idealized C_{2v} structures of (BDI)M(HE)$_2$, quantified by angle $\Delta\phi = |\phi_1 - \phi_2|$.

approximate C_s symmetry, with the mirror plane passing through the metal and the two E heteroatoms. The structures of **10** (Figure 1) and one of the two independent molecules of **13** (Figure 1, **13A**) illustrate this deformation; it can be quantified as the difference $\Delta\phi$ between the two QME angles, where Q is the midpoint of the BDI N–N vector (0° = no deformation).

The second deformation ("R") is a rotation of the piano stool E_2H_2M unit around its axis, relative to the BDI ligand (Figure 3), as clearly seen in the structure of **5** (Figure 1). In terms of heavy atoms only, this can be quantified as the angle χ between the NMN and EME planes (90° = no deformation).

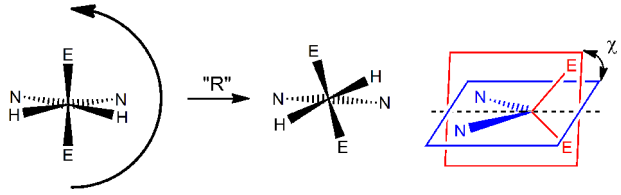

Figure 3. Schematic representation of R type deformation from idealized C_{2v} structures of (BDI)M(HE)$_2$, quantified by angle χ between NMN and EME planes.

The relevant quantities are given in Table 1. Inspection shows that the more hindered ^{Me}BDI and ^{Et}BDI complexes mostly show a T type deformation (**1**, **2**, **9**, **10**, **12**: $\Delta\phi$ = 13–19°, χ = 86–90°), whereas with the less bulky ^{MeO}BDI ligand the R type deformation is more prevalent (**3**, **5**, **8**, **11**: $\Delta\phi$ < 3°, χ = 67–75°). The calculated geometry reported for (F-BDI)Rh(HSiMe$_3$)$_2$[31] also fits in the latter category. The somewhat atypical stannane complex **7** shows both types of deformation ($\Delta\phi$ = 16°, χ = 75°). Interestingly, in mixed borane/silane complex **13** one of the two independent molecules shows a pure T type deformation ($\Delta\phi$ = 13°, χ = 90°), while the other shows less of the T type but instead a significant R deformation ($\Delta\phi$ = 8°, χ = 71°), suggesting that both deformations are comparatively easy. The fact that solution NMR spectra suggest higher symmetry (C_{2v} for **1**-**11**, C_s for **12** and **13**) proves that both distortions are easily reversible (Figure 4).

It seems likely that the preference of the bulky E groups for "up" and "down" positions is mainly steric. The ligand aryl "arms" strongly limit space within the plane of the (BDI)M fragment. In complex (^{iPr}BDI)IrH$_4$,[25] containing the smallest possible E groups, rotation of the piano stool bottom has proceeded over ~45°, all the way toward the alternative C_{2v} geometry:

DOI: 10.1021/acs.organomet.7b00469
Organometallics XXXX, XXX, XXX–XXX

Table 1. T and R Type Deformations of $(BDI)M(HE)_2$ Complexes[a]

complex	ligand	M	E	T: $\Delta\phi$ (deg)	R: χ (deg)
1[27]	^{Me}BDI	Rh	Si	17.0	88.9
2	^{Et}BDI	Rh	Si	13.5	89.5
3	^{MeO}BDI	Rh	Si	0.0	71.2
5	^{MeO}BDI	Rh	Ge	0.0	69.5
7	^{MeO}BDI	Rh	Sn	15.9	75.1
8	^{Me}BDI	Rh	B	2.4	67.0
9	^{Me}BDI	Ir	Si	13.9	87.8
10[b]	^{Et}BDI	Ir	Si	19.2	86.7
				18.2	88.7
				18.4	89.3
11	^{MeO}BDI	Ir	Si	0.0	75.3
12	^{Me}BDI	Rh	Sn/Si	14.9	90.0
13[c]	^{Me}BDI	Rh	Si/B	7.9	71.1
				−13.4	89.8
$(PyPyr)Rh(SiPh_3)_2$[32]				22.9	87.2
$(PyPyr)Rh(SiPh_2{}^tBu)_2$[32]				22.8	84.7
$(PyPyr)Rh(SiPh_3)_2$[32]				17.8	89.1

[a]For the meaning of angles $\Delta\phi$ and χ see the text and Figures 2 and 3. [b]Three independent molecules in unit cell. [c]Two independent molecules in unit cell.

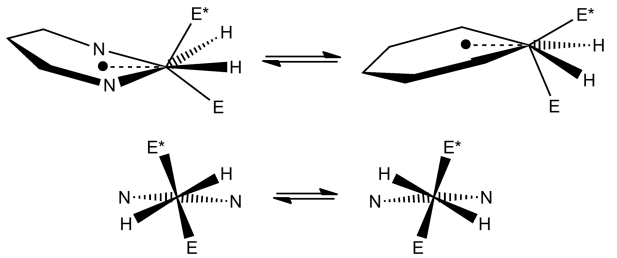

Figure 4. Reversibility of T and R deformations leading to effective C_{2v} symmetry.

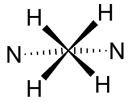

Using the same type of analysis, complexes $(PyPyr)M(HSiR_3)_2$[32] (included in Table 1) are found to exhibit clear T type deformations ($\Delta\phi$ = 18−23°). Also in that case, the observation of equivalent E groups implies easy reversibility.

A description as piano-stool complexes allows easy comparison of the $M(HE)_2$ fragments between Cp* and BDI complexes. Relevant data are collected in Table 2. The $Cp^*M(HE)_2$ complexes reported to date have more or less regular four-legged piano-stool geometries, with E−M−E angles in the range of 100−110° and H−M−H angles (where determined) somewhat smaller (80−100°). $(PyPyr)Ir(HSiPh_3)_2$[32] has a somewhat larger SiMSi angle of 116.10(4)°, presumably because there is little hindrance above and below the N_2Ir plane and/or because $HSiPh_3$ requires more space than $HSiEt_3$.

Like $Cp^*Rh(HBPin)_2$[19] and $Cp^*Rh(HBPin)(HSiEt_3)$,[18] HBPin complexes **8** and **13** show one short B−H contact per boron atom, while complexes of silanes, germanes, and stannanes do not have comparably short E−H contacts (after correction for differences in atomic radii). E−M−E angles vary over a range of 95−112°; for complexes with the same HE substrate the E−M−E angle is 5−10° smaller for $(BDI)M(HE)_2$ than for $Cp^*M(HE)_2$. The trend in H−M−H angles is less clear but this may be due to the large uncertainty in H atom positions. In any case, the E−M−E and H−M−H angles agree much better with the piano-stool interpretation than with a strongly distorted octahedral coordination (where an E−M−E angle closer to 180° would be expected).

Structure and Bonding: DFT Results. $Cp^*M(HE)_2$ and $(BDI)M(HE)_2$ complexes were studied by DFT: geometry optimization with Turbomole, def-TZVP basis, DFT-D3 dispersion corrections, and enthalpy and entropy corrections to free energies. For both Rh and Ir, a range of HE substrates was investigated in combination with the ligands Cp* and ^{Me}BDI. For the "benchmark" substrate $HSiMe_3$, a set of 10 ligands was studied. Dissociation free energies of the first and second HE substrate from the metal are collected in Tables 3 (substrate variation) and 4 (ligand variation).

$$LM(HE)_2 \xrightarrow{\Delta G_1} LM(HE) + HE$$

$$LM(HE) \xrightarrow{\Delta G_2} LM + HE$$

For most substrates, only a single local minimum was found for H−E coordination/oxidative addition. H−C bonds behave atypically, yielding usually separate local minima for σ-complex and oxidative addition product. In the following we focus on bonds other than H−C.

HE Dissociation Energies. Table 3 summarizes the variation in M−HE dissociation free energy as a function of the substrate HE. The calculated ΔG_1 value of 30.7 kcal/mol for $Cp^*Rh(HSiMe_3)_2$ agrees fairly well with the 28.1 kcal/mol reported for dissociation of $HSiEt_3$ from $Cp^*Rh(HSiEt_3)_2$.[22] The first HE dissociation energy varies fairly consistently in the order H_2 < HBPin ≈ $HSiMe_3$ ≈ $HGeMe_3$ < $HSnMe_3$. Binding to Ir is stronger than to Rh by about 10 kcal/mol, and Cp*M fragments have higher dissociation energies than (^{Me}BDI)M fragments by 10−15 kcal/mol. The second HE dissociation energy is larger than the first by 5−25 kcal/mol but shows roughly similar trends. Oxidative addition of H−C bonds is much less favorable than of the other H−E bonds, and dissociation (elimination) of the first H−C bond is consistently exergonic.

A more fine grained comparison is presented in Table 4, where binding of $HSiMe_3$ is collected for variously substituted ligands. For both ΔG_1 and ΔG_2, the trend is ^{Me}BDI ≈ ^{Et}BDI > ^{Me,iPr}BDI > ^{iPr}BDI ≈ ^{Me,tBu}BDI, reflecting increasing steric bulk of the ligands. Reducing the electron-donating power of the BDI ligand by introducing CF_3 groups at the imine positions decreases ΔG_1 and ΔG_2 (relative to ^{Me}BDI) by a few kcal/mol.[35] In contrast, strongly increased binding is observed with ^{MeO}BDI and BDI-F. Since electronic effects should work in the opposite direction, steric factors probably play a role here; this would be consistent with the observed/calculated structural deformations mentioned earlier. The strong HE binding to unsubstituted versions of (PyPyr)M fragments is also likely due to steric factors.

Degree of Oxidative Addition. The set of complexes studied here displays a near-continuous variation between the extremes of simple σ-complex formation (Chart 1A, formally M^I) and full oxidative addition (Chart 1B, formally M^V). HE bonding was analyzed for ^{Me}BDI and Cp* ligands in combination with Rh and Ir, on the basis of bond distances

DOI: 10.1021/acs.organomet.7b00469
Organometallics XXXX, XXX, XXX−XXX

Table 2. Piano-Stool Geometries (Å and deg) for Cp*M(HE)$_2$ and (BDI)M(HE)$_2$ Type Complexes[a]

compound	ref	M−E	M−H	E−H[d]	∠HMH	∠EME
Cp*Rh(HSiEt$_3$)$_2$[b]	6	2.379(2)	1.581(2)	2.212(2)	94.84(18)	107.90(8)
Cp*Rh(HBPin)$_2$	19	2.071(3)	1.49(3)	166(3)	88(2)	104.9(1)
Cp*Rh(HBPin)(HSiEt$_3$)	18	2.038(5) (B)	1.58(3)	1.74(4)	92(5)	102.6(2)
		2.368(2) (Si)		2.27(4)		
Cp*Ir(HSiEt$_3$)$_2$[b]	8	2.390(1)	1.594(2)	2.272(2)	99.50(16)	109.49(6)
(PyPyr)Ir(HSiPh$_3$)$_2$	32	2.333(1)	1.66(2)	2.26(3)	84(2)	116.10(4)
(^{iPr}BDI)IrH$_4$	25		1.47(2)		96(2)	
(^{Me}BDI)Rh(HSiEt$_3$)$_2$ (**1**)	27	2.3511(6)	1.51(2)	2.19(2)	96(2)	101.54(2)
(^{Me}BDI∧SiHEt$_2$)Rh(HSiEt$_3$) (**1′**)	27	2.3435(6)	1.50(2)	1.96(2)	92(1)	111.98(3)
(^{Et}BDI)Rh(HSiEt$_3$)$_2$ (**2**)	*c*	2.352(2)	1.38(3)	2.1(2)	94(2)	99.68(3)
(^{MeO}BDI)Rh(HSiEt$_3$)$_2$ (**3**)	*c*	2.353(1)	1.50(3)	1.99(3)	93(3)	105.46(6)
(^{MeO}BDI)Rh(HGeEt$_3$)$_2$ **5**	*c*	2.4308(7)	1.57(3)	2.13(3)	99(2)	104.31(3)
(^{MeO}BDI)Rh(HSn^{n}Bu$_3$)$_2$ (**7**)	*c*	2.563(1)	1.47(4)	2.27(4)	92(3)	104.89(2)
(^{Me}BDI)Rh(HBPin)$_2$ (**8**)	*c*	2.061(2)	1.53(2)	1.49(2)	94(1)	96.0(1)
(^{Me}BDI)Ir(HSiEt$_3$)$_2$ (**9**)	*c*	2.359(2)	1.4(1)	2.1(1)	98(5)	101.35(7)
(^{Et}BDI)Ir(HSiEt$_3$)$_2$ (**10**)	*c*	2.3601(4)	1.32(1)	2.14(1)	101(1)	102.23(2)
(^{MeO}BDI)Ir(HSiEt$_3$)$_2$ (**11**)	*c*	2.357(1)	1.47(4)	2.17(4)	103(3)	106.84(5)
(^{Me}BDI)Rh(HSiEt$_3$)(HSn^{n}Bu$_3$) (**12**)	*c*	2.356(1) (Si)	1.57(3)	2.06(3)	98(2)	97.31(3)
		2.6005(8) (Sn)		2.54(3)		
(^{Me}BDI)Rh(HSiEt$_3$)(HBPin) (**13**)	*c*	2.035(2) (B)	1.48(2)	1.72(2)	96(1)	96.3(1)
		2.361(2) (Si)		2.11(2)		

[a]Corresponding bond lengths/angles are averaged; see Table S4 in the Supporting Information for all individual bond lengths/angles. [b]Combined X-ray + neutron diffraction structure determination. [c]This work. [d]Average over each E of its shortest E−H contact.

Table 3. First and Second HE Dissociation Free Energies (kcal/mol) from (^{Me}BDI)M(HE)$_2$ and Cp*M(HE)$_2$

	(^{Me}BDI)Rh		(^{Me}BDI)Ir		Cp*Rh		Cp*Ir	
HE	ΔG_1	ΔG_2	ΔG_1	ΔG_2	ΔG_1	ΔG_2	ΔG_1	ΔG_2
H_2	13.0[a]	15.4[a]	22.2	28.3	17.9	26.9	26.9	52.1
HBPin	17.2	26.9	30.1	39.6	26.8	32.4	35.1	56.6
$HSiMe_3$	15.8	28.7	26.6	44.6	30.7	34.4	38.9	58.5
$HGeMe_3$	19.6	28.6	29.3	43.7	32.7	37.7	39.8	61.5
$HSnMe_3$	28.2	30.3	39.5	42.8	40.3	41.5	47.0	63.8
HMe	N/A[b]	−2.1	−8.0	12.2	−10.0	14.6	−3.7	41.3

[a]These are dihydrogen complexes. [b]Bis-HMe adduct not a local minimum.

Table 4. First and Second $HSiMe_3$ Dissociation Free Energies (kcal/mol) of (BDI)M($HSiMe_3$)$_2$ and Cp*M($HSiMe_3$)$_2$

	Rh		Ir	
ligand	ΔG_1	ΔG_2	ΔG_1	ΔG_2
^{Me}BDI	15.8	28.7	26.6	44.6
^{Et}BDI	15.0	30.3	26.5	45.7
^{iPr}BDI	8.5	24.2	19.7	40.0
^{Me,iPr}BDI	13.2	27.3	24.9	42.8
^{Me,tBu}BDI	4.2	23.7	15.7	40.2
^{MeO}BDI	23.1	33.7	33.3	50.9
F-BDI	22.3	35.1	32.8	52.9
^{Me}BDI-CF_3	12.4	25.2	23.9	40.7
PyPyr[a]	27.1	36.5	38.3	53.2
Cp*	30.7	34.4	38.9	58.5

[a]See ref 32. Calculations were done for a model ligand without Ph substituents.

(M−E, M−H, and H−E) as well as the corresponding Wiberg bond indexes (WBIs, Table 5). The Cp* systems are nearly all best described as M^V with mostly complete oxidative addition; M−H WBIs are ∼0.6 while H−E bond indexes are on the order of 0.1, in good agreement with the values of 0.12−0.21 reported by the Crimmin group for these residual interactions.[22] The only exceptions are the HBPin complexes, for which Hartwig et al. already reported short B−H distances and significant B−H interactions.[19] We obtain a WBI of 0.35 for the short B−H contacts, with an M−H WBI of 0.44, suggesting a position close to the middle of the oxidative-addition scale; the experimental H atom positions[18,19] also agree with this picture. The Ir analogue, however, is predicted to be much closer to full oxidative addition, with an H−E WBI of only 0.17 and an M−H WBI of 0.55.

The WBI data indicate a systematic shift toward less complete oxidative addition on moving from Cp* to ^{Me}BDI complexes: H−E WBIs become larger and M−E and M−H WBIs become smaller. The trend of less complete addition for Rh is retained. The most extreme case is (^{Me}BDI)Rh(H_2)$_2$, which is predicted to be a bis(dihydrogen) complex, while both Cp*RhH_4 and (^{Me}BDI)IrH_4 are still true tetrahydrides. (^{Me}BDI)Rh(HBPin)$_2$ is closer to the σ-complex side of the scale, while (^{Me}BDI)Ir(HBPin)$_2$ is closer to the oxidative-

DOI: 10.1021/acs.organomet.7b00469
Organometallics XXXX, XXX, XXX−XXX

Table 5. Wiberg Bond Indexes for $M(HE)_2$ Cores and Derived OA Values (Eq 1)[a]

	Cp*Rh				Cp*Ir			
HE	M−E	M−H	H−E[b]	OA	M−E	M−H	H−E[b]	OA
H_2	0.64	0.64	0.09	82	0.66	0.66	0.08	84
HBPin	0.58	0.44	0.35	57	0.66	0.55	0.17	72
$HSiMe_3$	0.52	0.57	0.12	74	0.58	0.60	0.10	77
$HGeMe_3$	0.52	0.58	0.12	74	0.57	0.60	0.10	77
$HSnMe_3$	0.49	0.61	0.11	76	0.54	0.64	0.09	79
HMe	0.68	0.61	0.10	79	0.69	0.65	0.08	83
	(^{Me}BDI)Rh				(^{Me}BDI)Ir			
HE	M−E	M−H	H−E[b]	OA	M−E	M−H	H−E[b]	OA
H_2	0.35	0.35	0.56	35	0.64	0.64	0.18	75
HBPin	0.54	0.36	0.47	46	0.70	0.51	0.25	66
$HSiMe_3$	0.50	0.51	0.20	66	0.60	0.59	0.12	76
$HGeMe_3$	0.48	0.51	0.24	65	0.58	0.60	0.12	76
$HSnMe_3$	0.46	0.56	0.17	70	0.53	0.63	0.12	77
HMe	c				0.75	0.64	0.15	79
	(PyPyr)Rh				(PyPyr)Ir			
HE	M−E	M−H	H−E[b]	OA	M−E	M−H	H−E[b]	OA
$HSiMe_3$	0.50	0.55	0.24	67	0.61	0.62	0.12	77

[a]Averaged over C_2 symmetry. [b]Largest of H−E and H−E′ values. [c]HMe adduct is not a local minimum.

addition side. As a rough indication of the degree of oxidative addition we suggest the use of a quantity OA defined by eq 1:

$$\mathrm{OA} = \left(1 - \frac{W_{\mathrm{H-E}} + W_{\mathrm{H-E'}}(\mathrm{complex})}{W_{\mathrm{H-E}}(\mathrm{free})}\right) \times 100\% \quad (1)$$

which is based on the loss of net H−E bonding due to coordination and oxidative addition; Table 5 includes the resulting OA values.[36] Crabtree et al. have mapped out a path for oxidative addition of a C−H bond to a metal center on the basis of relevant X-ray structures.[37] Their conclusion was that the reaction path is highly curved, starting with approach of the hydrogen atom to the metal center and only involving side-on interaction at a later stage. This is likely to apply to other E−H bonds as well;[38,39] thus, the OA value we proposed probably does not represent a linear scale. However, it at least allows us to put complexes with different supporting ligands and HE substrates on a common scale. Figure 5 shows calculated core geometries and individual WBIs for the four HBPin complexes, which show one of the largest ranges of OA values.

In summary, we conclude that Cp*M$(HE)_2$ and (BDI)M$(HE)_2$ complexes show strong analogies. Oxidative addition progresses further for Cp* than for BDI and more for Ir than for Rh. With HBPin oxidative addition does not progress as far as with H−Si, H−Ge, and H−Sn bonds. Sterics play an important role, as noted earlier by the Tilley group.[32]

A Stannane-Functionalized Ligand? The path previously proposed for the rearrangement of **1** to **1′**,[27] on the basis of DFT calculations, involves initial dissociation of $HSiEt_3$, cleaving of one Si−C bond, benzylic ligand C−H activation, elimination of ethane, formation of a new Si−C bond, and recapture of previously dissociated $HSiEt_3$.

As mentioned above, we never observed a similar rearrangement of HSn^nBu_3 complexes. This might be due to the high dissociation energy of stannanes from (^{R}BDI)M$(HSnR_3)_2$ (Table 3). Attempts using substoichiometric amounts of HSn^nBu_3 to avoid formation of the bis(stannane) adduct resulted in incomplete conversion and messy reaction mixtures.

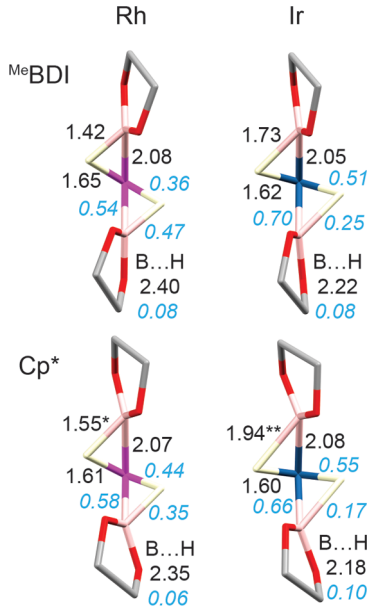

Figure 5. Optimized M$(HBPin)_2$ core geometries for (^{Me}BDI)M$(HBPin)_2$ and Cp*M$(HBPin)_2$ complexes: C_2-averaged bond lengths (Å) and Wiberg bond indexes (in blue and italics). Distances marked with asterisks show significant deviations from C_2 symmetry: (*) 1.51/1.60 Å; (**) 1.89/1.98 Å.

One way to avoid this problem might be to start with organotin compounds not containing any Sn−H bonds. We observed that (^{Me}BDI)Rh(COE)(N_2) reacts with $SnMe_4$, but the reaction is not very clean and produces a mixture of as yet unidentified compounds. However, if the reaction is carried out in the presence of H_2 (with Rh:Sn ≈ 1:4), NMR indicates formation of a mixture of two complexes (**14** and **14′**) and free ligand in the approximate ratio 1:1.2:0.8. So far we have been unable to separate these, and characterization is thus mostly based on NMR.[40] Both contain two hydrogens bound to Rh. In compound **14**, the hydrogens are equivalent at all temperatures

DOI: 10.1021/acs.organomet.7b00469
Organometallics XXXX, XXX, XXX−XXX

studied, and they show equal coupling to the two tin atoms. The ligand skeleton has effective C_{2v} symmetry, and we believe the most reasonable assignment for this complex is (^{Me}BDI)-Rh(HSnMe$_3$)$_2$. Complex **14′** shows two strongly broadened hydride signals at room temperature which on cooling sharpen to reveal coupling patterns (Figure 6). On heating the broad

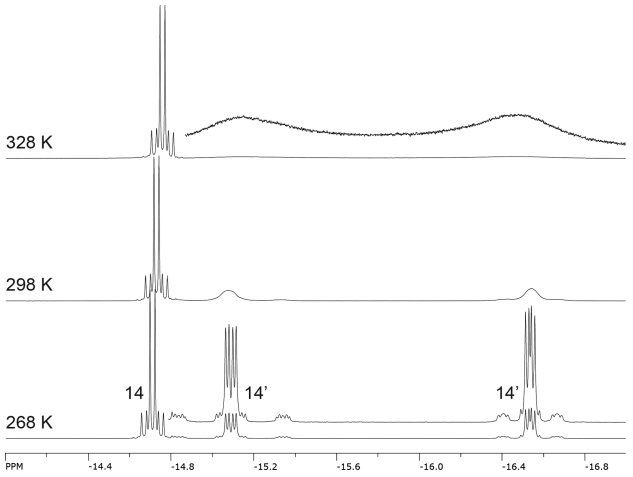

Figure 6. Hydride region of 500 MHz ^{1}H NMR spectra of a mixture of **14** and **14′** in THF-d_8.

signals broaden even further, while all other ^{1}H signals remain sharp. Both hydrides of **14′** couple to Rh, to each other, and to two tin atoms. The H−H and Rh−H couplings are comparable to those reported previously for the ligand-functionalized HSiEt$_3$ complex **1′** (which was not fluxional). The ligand skeleton does not appear to have any symmetry, and one of the expected aryl methyl groups is missing, while a tin-bound CH$_2$ group has been formed. Even though a full assignment of all signals of this compound in the product mixture (see the Experimental Section and Figures S37 and S38 in the Supporting Information) is tentative at this point, it seems plausible that complex **14′** is the ligand-functionalized version of **14**. In support of this, ESI-MS of the mixture in THF (see Figures S44−S47 in the Supporting Information) shows peaks corresponding to the ions (M + H)$^+$ expected for **14**, **14′**, and free ligand, with the expected isotope patterns, and HR-MS measurements confirm the proposed compositions of these ions.

The core geometries of **14** and **14′** could be expected to be rather similar (cf. the similar cores of **1** and **1′**[27]), except that any dynamic T or R type deformation in **14** would be frozen out by the BDI−Sn connection in **14′**. The observed J_{SnH} of 41 Hz for **14** represents C_{2v}-averaged values. Assuming that $^1J_{SnH}$ and $^2J_{SnH}$ have opposite signs,[34] the corresponding C_{2v}-averaged J_{SnH} value for **14′** is 79 Hz,[41] i.e. significantly larger than for **14**, suggesting that the ligand-functionalized complex **14′** has somewhat higher σ-stannane character, although the calculated structure and WBI indicate that the dominant description is still that of a dihydride (see also Figure S48 in the Supporting Information).

Calculations indicate the observed fluxionality can be explained by a dihydride−dihydrogen equilibrium as shown in Scheme 2. In the rate-limiting step, the hydride closest to the functionalized ligand arm moves between the tin atoms to the other hydride, forming the H$_2$ complex; this step bears some similarity to the H migration path identified by DFT for silyl

Scheme 2. Calculated Profile for Proposed Mechanism for Hydride Exchange in 14′: Free Energies (298 K, 1 bar) in kcal/mol

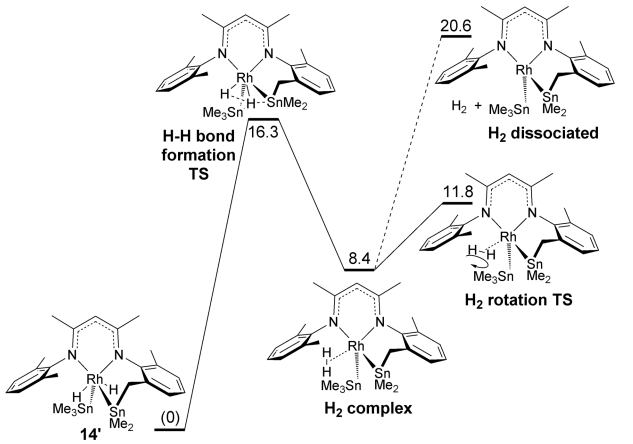

exchange in CpRhH(silyl)$_3$.[15] Our calculated activation parameters ($\Delta H^‡$ = 17.2 kcal mol^{-1}, $\Delta S^‡$ = 2.8 cal mol^{-1} K^{-1}) agree very well with those obtained from an Eyring plot ($\Delta H^‡$ = 18 ± 1 kcal mol^{-1}, $\Delta S^‡$ = 10 ± 3 cal mol^{-1} K^{-1}), confirming the intramolecular nature of the process. Calculated energies and geometries along the exchange path are shown in Figure S52 in the Supporting Information.

Dihydrogen complexes are often characterized by short T_1(min) values,[42,43] typically <160 ms at 500 MHz. We performed temperature-dependent T_1 determinations for the hydride signals of the **14**/**14′** mixture (for details see the Supporting Information). All three signals show a slow, smooth decrease in T_1 with temperature (+50 → −50 °C) to asymptotic values between 700 and 1100 ms, well within the criterion of >300 ms accepted for regular dihydrides. The negligible contribution from a dihydrogen complex structure agrees with the energy profile in Scheme 2, according to which the expected time fraction spent as a H$_2$ complex is ∼4 × 10^{-7} at 298 K.

Formation of complexes **14** and **14′** can be rationalized by assuming the same types of steps invoked earlier for ligand functionalization, complemented by Sn−C and H−H oxidative addition. A possible sequence of steps is shown in Scheme 3. SnMe$_4$ first adds to "(^{Me}BDI)Rh". Addition of H$_2$ and elimination of methane lead to (^{Me}BDI)Rh(H)(SnMe$_3$). From here, a second series of SnMe$_4$ oxidative addition, methane elimination, and H$_2$ addition produces **14**. Alternatively, (^{Me}BDI)Rh(H)(SnMe$_3$) could first undergo intramolecular ligand functionalization analogous to the **1** → **1′** transformation, followed by the same steps of SnMe$_4$ oxidative addition, methane elimination, and H$_2$ addition to finally produce **14′**. In agreement with this competition between intra- and intermolecular reactivity, experiments using a larger excess of SnMe$_4$ (Rh:Sn ≈ 1:8) produced less **14′** (**14**:**14′**:free ligand ≈ 1:0.3:0.4), whereas the use of less SnMe$_4$ led to extensive decomposition.

Limits of Steric Hindrance. Steric hindrance appears to be a key factor in controlling reactivity with HE substrates. To explore the limits of steric hindrance, we tested the reaction of (^{Me}BDI)Rh(COE) with 2 equiv of the bulky PPh$_3$ ligand. Molecular models indicate that two PPh$_3$ ligands would definitely not fit at Rh in a (^{R}BDI)Rh fragment. The reaction of (^{Me}BDI)Rh(COE) with PPh$_3$ in THF initially produces a

DOI: 10.1021/acs.organomet.7b00469
Organometallics XXXX, XXX, XXX−XXX

Scheme 3. Possible Pathways for the Reaction of "(^{Me}BDI)Rh" with $SnMe_4$ and H_2 To Give 14 and 14′[a]

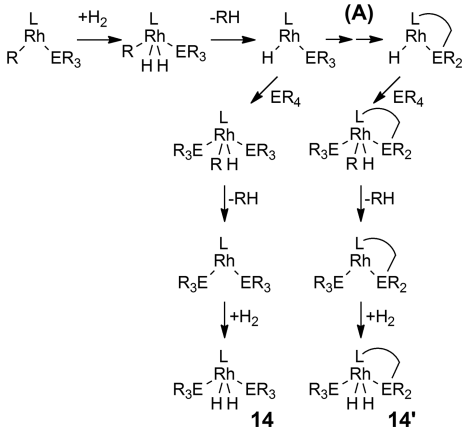

[a]The ligand functionalization sequence labeled A would follow the same path as the **1** → **1′** transformation.

brownish suspended solid which we have not yet been able to characterize. Over time (days) this solid converts to a final product (still suspended) that according to ^{31}P NMR (in benzene-d_6) contains two inequivalent PPh_3 ligands bound to Rh(I). A crystal structure determination showed that the ligand had tautomerized, forming an allyl moiety η^3-bound to Rh (**15**; see Scheme 4 and Figure S14 in the Supporting Information).

Scheme 4. Reaction of (^{Me}BDI)Rh(COE)with PPh_3

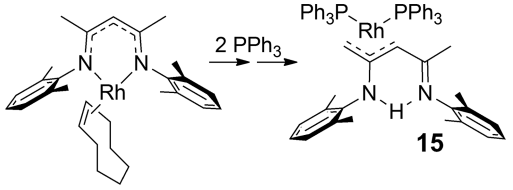

A fair number of complexes of C-deprotonated BDI ligands have been reported,[44−61] but to the best of our knowledge this is the first example where a single metal atom prefers to bind to the carbon backbone of such a ligand rather than to its nitrogen atoms. This rearrangement may be an indication of the nature of decomposition pathways occurring in reactions of (^{R}BDI)-Rh(COE) with bulky HE substrates or other ligands.

CONCLUSIONS

A combined experimental and computational study has revealed strong similarities between Cp*M and (BDI)M fragments (M = Rh, Ir) in their interaction with H−E compounds (silanes, germanes, stannanes, boranes) to give $LM(HE)_2$ complexes. There appears to be for these compounds a near-continuous scale from mostly σ-complex type to full oxidative addition. In general, BDI complexes feature less complete oxidative addition of the H−E bonds to the metal, and Rh complexes show a lower degree of oxidative addition than Ir complexes. Cp*Ir shows the strongest bonds to substrates, while (BDI)Rh shows the weakest bonds. Substrate binding is rather sensitive to steric effects in both substrate and BDI ligand. The general trend is H_2 < HBPin < silanes ≈ germanes < stannanes.

The large dissociation energy of stannanes may be a factor limiting ligand functionalization with this class of substrates. We report evidence that it is possible to partially circumvent this issue and generate a stannane-functionalized BDI ligand by avoiding the use of free tin hydrides, but forming $HSnMe_3$ within the Rh coordination sphere from $SnMe_4$ and H_2.

EXPERIMENTAL SECTION

Syntheses. All syntheses (with the exception of the free ^{Me}BDI and ^{Et}BDI ligands) were performed under an inert atmosphere (argon) with Schlenk techniques or in a nitrogen-filled drybox. Solvents were distilled from Na/benzophenone. 2,6-Diethylaniline, acetylacetone, and *n*-butyllithium (1.6 M in hexanes) were purchased from Sigma-Aldrich and used as received. $[Rh(COE)_2Cl]_2$ was purchased from Strem Chemicals. $[Ir(COE)_2Cl]_2$ was prepared according to a literature procedure;[62] (^{R}BDI)H and (^{R}BDI)Li(THF) (R = MeO, Me, Et) were prepared according to the literature.[63] Syntheses of complexes **1**, **1′**, and **3**−**5** have been reported before.[27]

Elemental analyses was done by Guelph Chemical laboratories Ltd. Due to the "oily" nature of the complexes studied, even repeated crystallization did not always yield a material with perfect analysis. As additional evidence of purity, ^{1}H and ^{13}C NMR spectra of all new complexes are provided in the Supporting Information.

ESI-MS spectra were recorded at the Mass Spectrometry Facility of the University of Alberta (Edmonton, AB, Canada).

All NMR spectra were recorded on Bruker Avance 300 MHz and Bruker Avance III 500 MHz spectrometers. Spectra were run with $CDCl_3$, C_6D_6, $C_6D_5CD_3$, C_4D_8O, or C_6D_{12} as indicated and calibrated with the corresponding reference peaks (^{1}H, δ 7.26, 7.16, 2.08, 3.58, and 1.72 and 1.44 ppm; ^{13}C, δ 77.16, 128.06, 20.43, 67.21, and 25.31 and 27.58 ppm).[64] All chemical shifts are in ppm, and all *J* couplings and line widths (fwhm) are in Hz. VT-NMR spectra were simulated using gNMR.[65] The numbering used for the ^{R}BDI ligand is:

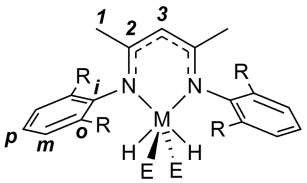

Synthesis of (^{Et}BDI)Rh($HSiEt_3$)$_2$ (2). A solution of (^{Et}BDI)Li-(THF) (100 mg, 0.23 mmol) in THF was added to a solution/suspension of $[Rh(COE)_2Cl]_2$ (81 mg, 0.12 mmol) in THF. All solids dissolved, producing a dark brown solution. All solvents were evaporated in vacuo, and the solid was extracted with hexane in a nitrogen-filled drybox. After removal of solids by centrifugation, $HSiEt_3$ (79 mg, 0.68 mmol) was added to the hexane solution, which was stirred for 5 min. Solvents were removed in vacuo, and the residue was crystallized from $^iPr_2O$ (+25 to −35 °C), producing a dark green crystalline solid. The mother liquor was removed, and the solid was washed with cold hexane and dried, leaving 0.066 g (42%) of **2**.

^{1}H NMR (THF-d_8, 300 MHz): δ 7.15−7.00 (6H, m, *m*, *p*), 5.22 (1H, s, 3), 2.7−2.9 (4H, m, $ArCH_2$), 2.4−2.6 (4H, m, $ArCH_2$), 1.70 (6H, s, 1), 1.24 (12H, t, *J* 7.6, $ArCH_2CH_3$), 0.70 (30H, br s, Si*Et*), −14.82 (2H, d, J_{Rh} 20.7, J_{Si} 9, Rh*H*). ^{13}C NMR (THF-d_8, 75 MHz): δ 160.8, 156.0 (2, *i*), 136.2 (*o*), 125.7 (*m*), 125.3 (*p*), 99.3 (J_{Rh} 1.1, 3), 25.5 ($ArCH_2$), 22.9 (1), 13.4 ($ArCH_2CH_3$), 13.0, 9.3 (Si*Et*). Anal. Calcd for $C_{37}H_{65}N_2RhSi_2$ (697.02): C, 63.76; H, 9.40; N, 4.02. Found: C, 63.53; H, 9.48; N, 3.87.

Synthesis of (^{MeO}BDI)Rh($HSiEt_3$)$_2$ (3). A solution of (^{MeO}BDI)-Li(THF) (50 mg, 0.16 mmol) in 0.4 mL of THF was added to a solution/suspension of $[Rh(COE)_2Cl]_2$ (49.2 mg, 0.08 mmol) in THF (0.5 mL). The mixture was stirred at room temperature for 10 min. $HSiEt_3$ (37.2 mg, 0.32 mmol) was added, and stirring was continued for 5 min. Solvents were removed in vacuo, and the residue was extracted with diethyl ether. Cooling to −35 °C produced a yellow crystalline solid. The mother liquor was removed, and the solid was washed with cold hexane and dried, leaving 0.035 g (45%) of **3**.

^{1}H NMR (THF-d_8, 500 MHz): δ 6.99 (2H, t, *J* 8.5, *p*), 6.57 (4H, d, *J* 8.5, *m*), 5.02 (1H, s, 3), 3.75 (12H, s, O*Me*), 1.65 (6H, s, 1), 0.63−0.78 (15H, m, *Et*), −14.67 (2H, d, J_{Rh} 21.0, J_{Si} 10, Rh*H*). ^{13}C NMR

DOI: 10.1021/acs.organomet.7b00469
Organometallics XXXX, XXX, XXX−XXX

(THF-d_8, 125 MHz): δ 161.4 (2), 153.6 (*o*), 138.0 (*i*), 124.8 (*p*), 104.2 (*m*), 98.6 (J_{Rh} 1.6, 3), 55.1 (O*Me*), 23.2 (1), 11.7, 9.3 (*Et*). Anal. Calcd for $C_{33}H_{57}N_2O_4RhSi_2$ (704.90): C, 56.23; H, 8.15; N, 3.97. Found: C, 55.66; H, 8.17; N, 3.97.

Synthesis of (^{MeO}BDI)Rh(HGeEt$_3$)$_2$ (5). In a N_2-filled drybox, $[Rh(COE)_2Cl]_2$ (0.0625 g, 0.174 mmol) was weighed into a small vial and dissolved in dry THF (3 mL) to form an orange solution. (^{MeO}BDI)Li(THF) (0.0780 g, 0.174 mmol) was weighed into another vial and dissolved in dry THF (3 mL). These two solutions were combined to form a red solution. This solution was transferred into a 25 mL Schlenk tube, and $HGeEt_3$ (59 μL, 0.348 mmol, 2.0 equiv) was added. Evolution of gas (N_2) was observed. After the mixture was stirred for 15 min at room temperature, all solvents were evaporated and the brown solid residue was extracted with 5 mL of Et_2O. After centrifugation, the red solution was layered with 5 mL of hexane and cooled to −35 °C overnight, producing a crystalline solid. The mother liquor was pipetted off, and the solids were washed with cold pentane and dried, leaving 0.052 g (40%) of **5**.

^{1}H NMR (THF-d_8, 500 MHz): δ 6.99 (2H, t, *J* 8.4, *p*), 6.58 (4H, d, *J* 8.4, *m*), 5.04 (1H, s, 3), 3.75 (12H, s, O*Me*), 1.67 (6H, s, 1), 0.77−0.88 (15H, m, *Et*), −15.02 (2H, d, J_{Rh} 14.5, Rh*H*). ^{13}C NMR (THF-d_8, 125 MHz): δ 161.0 (2), 153.5 (*o*), 138.8 (*i*), 124.6 (*p*), 104.3 (*m*), 98.6 (J_{Rh} 1.6, 3), 55.2 (O*Me*), 23.1 (1), 13.3, 10.3 (*Et*). Anal. Calcd for $C_{33}H_{57}Ge_2N_2O_4Rh$ (794.00): C, 49.92; H, 7.24; N, 3.53. Found: C, 50.18; H, 7.11; N, 3.68.

Attempted Synthesis of (^{Me}BDI)Rh(HSn^{n}Bu$_3$)$_2$ (6). A solution of (^{Me}BDI)Li(THF) (50 mg, 0.16 mmol) in 0.4 mL of THF was added to a stirred suspension of $[Rh(COE)_2Cl]_2$ (49.2 mg, 0.08 mmol) in THF. After 10 min, HSn^{n}Bu$_3$ (140 mg, 0.48 mmol) was added and the mixture was stirred for another 5 min. After evaporation of the solvent, ^{1}H NMR showed the presence of product **6** and free ligand in an approximately 4:1 ratio as well as some remaining COE. Purification attempts failed due to the high and similar solubilities of the various Sn^{n}Bu$_3$ compounds. The same reaction executed with a very large excess of HSn^{n}Bu$_3$ produced a mixture containing **6** and free ligand in a 1:1.2 ratio. Again, attempts at purification failed. ^{1}H NMR spectra for both reactions are included in the Supporting Information.

^{1}H NMR (benzene-d$_6$, 300 MHz), tentative assignments: δ 6.9−7.1 (m, *m*, *p*), 5.23 (1H, s, 3), 2.33 (12H, s, *o-Me*), −15.03 (2H, d, J_{Rh} 11, J_{Sn} 22, Rh*H*).

Synthesis of (^{MeO}BDI)Rh(HSn^{n}Bu$_3$)$_2$ (7). A solution of (^{MeO}BDI)-Li(THF) (75 mg, 0.199 mmol) in 0.4 mL of THF was added to stirred suspension of $[Rh(COE)_2Cl]_2$ (62 mg, 0.099 mmol) in THF. After 10 min, HSn^{n}Bu$_3$ (121.6 mg, 0.398 mmol) was added. After 5 min more, the solution was evaporated to dryness. Crystallization from Et_2O at −35 °C took a long time (months) but eventually gave large orange crystals.

^{1}H NMR (THF-d_8, 500 MHz): δ 6.98 (2H, t, *J* 8.4, *p*), 6.59 (4H, d, *J* 8.4, *m*), 5.11 (1H, s, 3), 3.78 (12H, s, O*Me*), 1.67 (6H, s, 1), 1.15−1.35 (24H, m, C−C*H*$_2$-C), 0.86−0.92 (30H, m, SnC*H*$_2$ and CH$_2$C*H*$_3$), −15.34 (2H, d, J_{Rh} 12, J_{Sn} 23, Rh*H*). ^{13}C NMR (THF-d_8, 125 MHz): δ 160.4 (2), 153.1 (*o*), 140.0 (*i*), 124.5 (*p*), 104.6 (*m*), 99.2 (br, 3), 55.6 (O*Me*), 30.3 (J_{Sn} 18, CH_2CH_3), 28.4 (J_{Sn} 70, $SnCH_2CH_2$), 22.7 (1), 17.1 (J_{Rh} 2, $SnCH_2$), 14.0 (CH_2CH_3). Anal. Calcd for $C_{45}H_{81}N_2O_4Sn_2Rh$ (1054.46): C, 51.26; H, 7.74; N, 2.66. Found: C, 51.48; H, 7.88; N, 2.71.

Synthesis of (^{Me}BDI)Rh(HBPin)$_2$ (8). In a N_2-filled drybox, $[Rh(COE)_2Cl]_2$ (0.20 g, 0.55 mmol) was weighed into a small vial. (^{Me}BDI)Li(THF) (0.21 g, 0.55 mmol) was weighed into a 25 mL Schlenk tube and dissolved in 10 mL of dry THF. The solution was added to the $[Rh(COE)_2Cl]_2$. After all solids had dissolved, the resulting dark brown solution was transferred back into the Schlenk tube. Solvent was evaporated in vacuo, the dark purple solid was extracted with hexane in a N_2-filled drybox, and solids were removed by centrifugation. A 0.25 mL portion of HBPin (1.67 mmol, 3.0 equiv) was added. After 5 min of stirring at room temperature, the mixture was evaporated to dryness. The residue was washed with hexane; the remaining solid was dissolved in THF/hexane (1/3) and cooled to −35 °C, producing a yellow crystalline solid. The mother liquor was removed, and the solid was washed with cold hexane, leaving 0.164 g (44%) of **8**. The compound decomposes in solution at room temperature in about 1 day.

^{1}H NMR (cyclohexane-d_{12}, 500 MHz): δ 6.94 (4H, d, *J* 7.4, *m*), 6.84 (2H, t, *J* 7.4, *p*), 5.15 (1H, s, 3), 2.37 (12H, s, *o-Me*), 1.72 (6H, s, 1), 1.06 (24H, s, BPin *Me*), −13.36 (2H, br d (fwhm 33), J_{Rh} 25, Rh*H*). ^{13}C NMR (cyclohexane-d_{12}, 125 MHz): δ 160.9, 158.8 (2 and *i*), 133.4 (*o*), 129.3 (*m*), 125.7 (*p*), 99.5 (J_{Rh} 2.5, 3), 84.5 (OC), 26.0 (BPin *Me*), 23.9 (1), 21.3 (*o-Me*). ^{11}B NMR (cyclohexane-d_{12}): δ 33.8. Anal. Calcd for $C_{33}H_{51}B_2N_2O_4Rh$ (664.30): C, 59.67; H, 7.74; N, 4.22. Found: C, 59.52; H, 7.77; N, 3.94.

Synthesis of (^{Me}BDI)Ir(HSiEt$_3$)$_2$ (9). A solution of (^{Me}BDI)Li-(THF) (75 mg, 0.24 mmol) in 2 mL of THF was added to a stirred solution of $[Ir(COE)_2Cl]_2$ (84 mg, 0.120 mmol) and excess $HSiEt_3$ (167 mg, 1.44 mmol) in 0.5 mL of diethyl ether. All solvents were evaporated in vacuo, and the solid was extracted with pentane in a nitrogen-filled drybox. Solids were removed by centrifugation, and the pentane solution was cooled to −35 °C. After 3 days, a single large yellow crystal had formed. The mother liquor was removed, and the solid was washed with cold hexane and dried, leaving 0.031 g (22%) of **9**.

^{1}H NMR (THF-d_8, 300 MHz): δ 7.06 (4H, d, J 7.3, *m*), 6.91 (2H, t, J 7.4, *p*), 5.54 (1H, s, 3), 2.21 (12H, s, *o-Me*), 1.74 (6H, s, 1), 0.5−0.8 (30H, m, Si*Et*), −16.33 (2H, s, J_{Si} not resolved, Ir*H*). ^{13}C NMR (THF-d_8, 75 MHz): δ 160.2, 157.7 (2, *i*), 131.0 (*o*), 129.0 (*m*), 125.6 (*p*), 102.6 (3), 22.7 (1), 19.9 (*o-Me*), 13.1, 9.5 (Si*Et*). Anal. Calcd for $C_{33}H_{57}N_2Si_2Ir$ (730.21): C, 54.28; H, 7.87; N, 3.84. Found: C, 54.05; H, 7.64; N, 3.96.

Synthesis of (^{Et}BDI)Ir(HSiEt$_3$)$_2$ (10). A solution of (^{Et}BDI)Li-(THF) (75 mg, 0.170 mmol) in 2 mL of THF was added to a stirred solution of $[Ir(COE)_2Cl]_2$ (60 mg, 0.085 mmol) and excess $HSiEt_3$ (60 mg, 0.51 mmol) in 0.4 mL of benzene. All solvents were evaporated in vacuo, and the solid was extracted with ^{i}Pr$_2$O in a nitrogen-filled drybox. After centrifugation, the ^{i}Pr$_2$O solution was cooled to −35 °C, forming a yellow crystalline solid. The mother liquor was removed, and the solid was washed with cold hexane and dried, leaving 0.044 g (33%) of **10**.

^{1}H NMR (THF-d_8, 300 MHz): δ 7.0−7.2 (6H, m, *m*, *p*), 5.48 (1H, s, 3), 2.7−2.9, 2.4−2.6 (4H each, m, ArC*H*$_2$), 1.76 (6H, s, 1), 1.24 (12H, t, *J* 7.5, ArCH$_2$C*H*$_3$), 0.6−0.7 (30H, m, Si*Et*), −16.48 (2H, s, J_{Si} not resolved, Ir*H*). ^{13}C NMR (THF-d_8, 75 MHz): δ 160.4, 156.5 (2, *i*), 135.9 (*o*), 126.0 (*p*), 125.6 (*m*), 102.7 (3), 25.2 (ArCH$_2$), 22.9 (1), 13.2 (ArCH$_2$CH$_3$), 13.0, 9.5 (Si*Et*). Anal. Calcd for $C_{37}H_{65}N_2Si_2Ir$ (786.32): C, 56.52; H, 8.33; N, 3.56. Found: C, 56.23; H, 8.09; N, 3.69.

Synthesis of (^{MeO}BDI)Ir(HSiEt$_3$)$_2$ (11). A solution of (^{MeO}BDI)-Li(THF) (15 mg, 0.040 mmol) in 2 mL of THF was added to a stirred solution of $[Ir(COE)_2Cl]_2$ (14 mg, 0.020 mmol) and excess $HSiEt_3$ (30 mg, 0.24 mmol) in 0.4 mL of benzene. Evaporation of the solvent, extraction, and crystallization from ^{i}Pr$_2$O gave a light yellow crystalline solid.

^{1}H NMR (THF-d_8, 500 MHz): δ 6.99 (2H, t, *J* 8.4, *p*), 6.60 (4H, d, *J* 8.4, *m*), 5.33 (1H, s, 3), 3.74 (12H, s, O*Me*), 1.70 (6H, s, 1), 0.66 (15H, s, *Et*), −16.24 (2H, s, J_{Si} not resolved, Ir*H*). ^{13}C NMR (THF-d_8, 125 MHz): δ 161.0 (2), 153.3 (*o*), 138.7 (*i*), 125.6 (*p*), 103.9 (*m*), 101.9 (3), 55.0 (O*Me*), 23.3 (1), 11.9, 9.3 (*Et*). Anal. Calcd for $C_{33}H_{57}N_2O4Si_2Ir$ (794.21): C, 49.91; H, 7.23; N, 3.53. Found: C, 49.62; H, 7.22; N, 3.39.

Synthesis of (^{Me}BDI)Rh(HSiEt$_3$)(HSn^{n}Bu$_3$) (12). A mixture of (^{Me}BDI)Rh(COE)(N_2) (79 mg, 0.145 mmol) and $HSiEt_3$ (37 mg, 0.32 mmol) in hexane was stirred for 10 min at room temperature. HSn^{n}Bu$_3$ (46 mg, 0.16 mmol) was added, and the mixture was stirred for another 30 min. All solvents were removed in vacuo, and the residue was extracted with Et_2O at −35 °C, yielding a red crystalline solid. The mother liquor was removed, and the solid was washed with cold hexane and dried, leaving 0.036 g (31%) of **12**.

^{1}H NMR (THF-d_8, 300 MHz): δ 7.06, 6.99 (2H each, d, *J* 7.2, *m*), 6.90 (2H, t, *J* 7.4, *p*), 5.26 (1H, s, 3), 2.41, 2.00 (6H each, s, *o-Me*), 1.67 (6H, s, 1), 1.10−1.55 (18H, m, C*H*$_2$C*H*$_2$C*H*$_2$), 0.89 (9H, t, *J* 7.2, *Me*(Bu)), 0.3−0.5 (15H, m, *Et*(Si)), −15.17 (2H, d, J_{Rh} 18, J_{Sn} 24, J_{Si} 8, Rh*H*). ^{13}C NMR (THF-d_8, 75 MHz): δ 160.3, 157.8 (2, *i*), 132.0,

DOI: 10.1021/acs.organomet.7b00469
Organometallics XXXX, XXX, XXX−XXX

129.4 (*o*, *o*′), 129.1, 128.9 (*m*, *m*′), 124.9 (*p*), 99.3 (J_{Rh} 1.8, 3), 30.5, 28.0 (CH_2(Bu)), 22.4 (1), 20.4 (*o-Me*), 19.7 (J_{Rh} 2, CH_2Sn), 19.5 (*o-Me*), 13.7 (*Me*(Bu)), 12.3 (CH_2Si), 8.3 (CH_3(Et)). Anal. Calcd for $C_{39}H_{69}N_2RhSiSn$ (816.33): C, 57.43; H, 8.53; N, 3.43. Found: C, 56.63; H, 8.45; N, 3.16.

Synthesis of (^{Me}BDI)Rh(HSiEt$_3$)(HBPin) (13). In a N_2-filled drybox, complex **1** (0.074 g, 0.11 mmol) was weighed into a small vial and dissolved in 5 mL of hexane. This hexane solution was placed in a second vial containing complex **8** (0.076 g, 0.11 mmol). After all of the solid had dissolved, the resulting clear yellow solution was transferred into a 25 mL Schlenk tube. The reaction mixture was evaporated to dryness, and 2 drops of Et_2O and 6 drops of hexane were added. The resulting solution was cooled to −35 °C overnight, but no solid was obtained. All solvents were evaporated, the residue was dissolved in 3 drops of hexane, and the resulting mixture was cooled to −35 °C. After 4 h, a solid had formed. The mother liquor was pipetted off, and the residue was washed with a small amount of cold hexane and dried, giving 0.020 g (27%) of **13**.

^{1}H NMR (cyclohexane-d_{12}, 500 MHz): δ 6.97 (4H, d, *J* 7.5, *m*), 6.86 (2H, t, *J* 7.5, *p*), 5.17 (1H, s, 3), 2.35 and 2.33 (6H each, s, *o-Me*), 1.74 (6H, s, 1), 1.03 (12H, s, BPin *Me*), 0.77 (m, 6H, SiCH_2), 0.70 (m, 9H, CH_2CH_3), −13.59 (2H, br d (fwhm 14), J_{Rh} 25.5, Rh*H*). ^{13}C NMR (cyclohexane-d_{12}, 125 MHz): δ 161.4, 159.0 (2 and *i*), 134.3, 131.2 (*o*), 129.7, 129.4 (*m*), 125.7 (*p*), 99.5 (J_{Rh} 1.6, 3), 84.7 (OC), 26.0 (BPin *Me*), 24.1 (1), 21.4, 21.0 (*o-Me*), 12.9, 10.2 (*Et*). ^{11}B NMR (cyclohexane-d_{12},): δ 34.7. Anal. Calcd for $C_{33}H_{54}BN_2O_2RhSi$ (652.60): C, 60.73; H, 8.34; N, 4.29. Found: C, 60.59; H, 8.11; N, 4.48.

Reaction of "(^{Me}BDI)Rh" with SnMe$_4$ and H$_2$ Giving 14/14′. In a nitrogen-filled drybox, a solution of (^{Me}BDI)Li(THF) (50 mg, 0.160 mmol) in THF was added to a solution/suspension of [Rh(COE)$_2$Cl]$_2$ (49 mg, 0.08 mmol) in THF. After the mixture was stirred for 5 min, all solvent was removed in vacuo and the solid was extracted with 5 mL of hexane. Solids were removed by centrifugation.

Note: conditions (volume of solvent, volume of Schlenk flask, timing) are critical for the success of the following reaction!

The hexane solution of (^{Me}BDI)Rh(COE)(N_2) was transferred into a 100 mL Schlenk flask. Me_4Sn (115 mg, 0.64 mmol) was added. The reaction flask was transferred to a hydrogen-filled Schlenk line, and the contents were stirred. The flask was opened and kept open for 1 min, letting hydrogen flow through it to replace much of the nitrogen. The flask was closed again but left connected to the hydrogen Schlenk line for 4 min more; then the connection to the Schlenk line was closed and the solution was stirred for 20 h at room temperature. Solvents were removed in vacuo, leaving a dark brown residue that according to NMR consisted of a mixture of **14**, **14**′, and free ligand (^{Me}BDI)H in the ratio 1:1.20:0.76 on the basis of ^{1}H NMR integration. Attempts to separate these compounds were unsuccessful. ESI-MS spectra of the mixture were recorded in positive ion mode through flow injection with freshly distilled THF; $(M + H)^+$ ions were detected for all three components. HR-MS: **14**, M = $C_{27}H_{46}N_2Rh^{120}Sn_2$, $(M + H)^+$ = 741.0766 (obsd), 741.0755 (calcd); **14**′, M = $C_{26}H_{42}N_2Rh^{120}Sn_2$, $(M + H)^+$ = 725.0453 (obsd), 725.0442 (calcd). For more details see Figures S44−S47 in the Supporting Information.

The same experiment as described above, but using double the amount of $SnMe_4$ (Rh:Sn = 1:8) produced more **14** but less **14**′ and free ligand (ratio 1:0.3:0.4 from integration of the ^{1}H NMR spectrum).

Tentative NMR assignments for the reaction mixture are as follows. ^{1}H NMR (THF-d_8, 300 MHz): complex **14**, δ (6.7−7.1 *m*, *p*), 5.35 (1H, s, 3), 2.20 (12H, s, *o-Me*), 1.74 (6H, s, 1), 0.11 (18H, s, J_{Sn} 50, SnMe_3), −14.73 (2H, d, J_{Rh} 12, J_{Sn} 41, Rh*H*); complex **14**′, δ (6.7−7.1 *m*, *p*), 5.32 (1H, s, 3), 2.39 (1H, d, *J* 10, SnCH_2), 2.34, 2.05, 1.99 (3H each, s, *o-Me*), 1.94 (1H, d, *J* 10, SnCH_2), 1.71, 1.66 (3H each, s, 1), 0.56 (3H, s, J_{Sn} 49, SnMe_2), 0.09 (3H, s, J_{Sn} 50, SnMe_2), −0.14 (9H, s, J_{Sn} 52, SnMe_3), −15.1 (1H, br, Rh*H*), −16.5 (1H, br, Rh*H*) (hydride signals at 263 K −15.09 (dd, 1H, J_H 8, J_{Rh} 18, J_{Sn} 258 and 49, Rh*H*), −16.54 (dd, 1H, J_H 8, J_{Rh} 14, J_{Sn} 134 and 29, Rh*H*); free (^{Me}BDI), δ 12.16 (1H, s, N*H*), (6.7−7.1 *m*, *p*), 4.92 (1H, s, 3), 2.14 (12H, s, *o-Me*), 1.66 (6H, s, 1). ^{13}C NMR (THF-d_8, 75 MHz): complex **14**, δ 160.3, 159.1 (2/*i*), 130.2 (*o*), 128.8 (*m*), 124.6 (*p*), 99.4 (J_{Rh} 2, 3), 22.5 (1), 19.8 (*o-Me*), 0.1 (J_{Rh} 2, J_{Sn} 303, SnMe_3); complex **14**′, δ 160.4, 159.5, 156.9, 155.6 (2/*i*), 135.7, 131.4, 129.9 (*o*), 129.3, 129.0, 127.1, 126.9 (*m*), 126.0 (*o*), 124.7, 123.0 (*p*), 100.0 (J_{Rh} 3, 3), 23.5 (SnCH_2), 22.4, 21.5 (1), 20.1, 19.0, 18.3 (*o-Me*), −1.8 (J_{Rh} 1, J_{Sn} 312, SnMe_3), −0.2 (J_{Rh} 2, SnMe_2), −2.7 (J_{Rh} 3, SnMe_2); free (^{Me}BDI)H, δ 161.3, 144.5 (2/*i*), 132.5 (*o*), 128.3 (*m*), 124.9 (*p*), 94.4 (3), 20.2 (1), 18.4 (*o-Me*).

Synthesis of (iso-^{Me}BDI)Rh(PPh$_3$)$_2$ (15). A solution of (^{Me}BDI)-Li(THF) (75 mg, 0.194 mmol) in THF was added to a solution/suspension of [Rh(COE)$_2$Cl]$_2$ (69 mg, 0.097 mmol) in THF. After all solids had dissolved to give a dark brown solution, the solvent was evaporated in vacuo and the solid was extracted with hexane in a nitrogen-filled drybox. After centrifugation, the hexane solution was added to a solution of PPh_3 (102 mg, 0.39 mmol) in hexane. After the mixture was stirred for 6 days at room temperature, the mother liquor was removed and the solid was washed with cold hexane and dried, leaving 0.08 g (44%) of **15**.

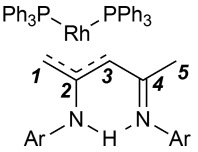

^{1}H NMR (benzene-d_6, 500 MHz): δ 10.23 (1H, s, N*H*), 7.7 (6H, m, PPh_3 *o*), 7.5 (6H, m, PPh_3 *o*), 6.8−7.0 (m, PPh_3 and Ar *m*,*p*), 3.33 (1H, d, *J* 5.5, 3), 2.78 (3H, s, *o-Me*), 2.57 (1H, dd, *J* 7.0, 4.0, 1), 2.42, 2.15 (3H each, s, *o-Me*), 1.67 (1H, ∼q, *J* 3.8), 1.49 (3H, s, *o-Me*), 0.81 (3H, s, 5). ^{13}C NMR (benzene-d_6, 125 MHz; assignments tentative): δ 176.4 (4), 150.6 (Ar *i*), 139.5 (d, J_P 24, PPh_3 *i*), 139.2 (d, J_P 20, PPh_3 *i*), 139.1 (Ar *i*), 137.7 (unresolved couplings, 2), 136.2, 135.9 (Ar *o*), 135.3 (d, J_P 14, PPh_3 *o*), 134.3 (d, J_P 13, PPh_3 *o*), 128.8 (Ar *o*?), 128.7 (PPh_3 *o*), 127.7 (d, J_P 9, PPh_3 *m*), 127.4 (d, J_P 10, PPh_3 *m*), 125.6, 122.5 (Ar *p*), 56.8 (dd, *J* 27, 7, 3), 44.6 (ddd, *J* 29, 9, 3, 1), 22.2 (5), 20.5, 19.4, 19.4, 19.0 (*o-Me*); remaining resonances obscured by C_6D_6 signal. ^{31}P NMR (benzene-d_6, 121 MHz): δ 51.2 (dd, J_{Rh} 214, J_P 31), 41.3 (dd, J_{Rh} 184, J_P 31). Anal. Calcd for $C_{57}H_{56}N_2P_2Rh$ (933.94): C, 73.31; H, 6.04; N, 3.00. Found: C, 72.99; H, 5.65; N, 2.70.

X-ray Structure Determinations. Crystal fragments were broken from large pieces of crystalline aggregate and sealed in thin glass capillaries. Each crystal in its capillary was mounted on a Bruker D8 three-circle diffractometer equipped with a rotating anode generator (Mo Kα X-radiation), multilayer optics incident beam path, and an APEX-II CCD detector. Data wee collected at a crystal to detector distance of 5 cm. Only for compound **9**, data were collected on a Bruker D8 QUEST ECO diffractometer: the crystal was mounted using a nylon loop under a cold stream of nitrogen (150 K).

Semiempirical absorption corrections (SADABS[66]) were applied and identical data merged. The unit-cell parameters were obtained by least-squares refinement on observed reflections with $I > 2\sigma(I)$. Structures were solved by direct methods (SHELXS[67]) and refined by full-matrix least-squares refinement (SHELXL[67]). Hydrogens were placed in calculated positions and refined in riding mode, except that metal-bound hydrides and the H(N) of complex **15** were freely refined. For compound **13**, there is a clear and severe disorder in the Et_3Si group of Si2. It was controlled using "SADI" to force its three Si−C and C−C bond lengths to be equal. Attempts to create an explicit disorder model failed. There may be additionally some minor disorder in the folding of the BPin five-membered rings. However, the (BDI)Rh cores of both independent molecules seem to be well-behaved. More complete details of all individual determinations are given in Table S1 in the Supporting Information.

Computational Details. All structures were fully optimized at the TPSSh[68]/def-TZVP[69] level using Turbomole[70] in combination with an external optimizer.[71,72] Vibrational analyses showed them to be minima (no imaginary frequencies) or transition states (exactly one imaginary frequency, corresponding to the reaction coordinate). These vibrational analyses were also used to calculate thermal corrections (enthalpy and entropy) at 298 K and 1 bar; the entropy contribution was scaled by 0.67 to account for reduced freedom in solution.[73,74] Dispersion corrections were calculated using Grimme's DFT-D3

DOI: 10.1021/acs.organomet.7b00469
Organometallics XXXX, XXX, XXX−XXX

method[75] ("-zero" damping) and were combined with the TZVP energies and thermal corrections to arrive at the final free energies. Wiberg bond indices were calculated using Gaussian 09[76] and the TZVP basis set[69] (LANL2DZ[77−79] on Rh and Ir).

■ ASSOCIATED CONTENT

Supporting Information

The Supporting Information is available free of charge on the ACS Publications website at DOI: 10.1021/acs.organomet.7b00469.

Crystallographic and spectroscopic details and computational results (PDF)

Cartesian coordinates of optimized structures (XYZ)

Accession Codes

CCDC 1557256, 1557259−1557262, 1557266, 1557268−1557269, 1557272−1557276, and 1557279 contain the supplementary crystallographic data for this paper. These data can be obtained free of charge via www.ccdc.cam.ac.uk/data_request/cif, or by emailing data_request@ccdc.cam.ac.uk, or by contacting The Cambridge Crystallographic Data Centre, 12 Union Road, Cambridge CB2 1EZ, UK; fax: +44 1223 336033.

■ AUTHOR INFORMATION

Corresponding Author

*E-mail for P.H.M.B.: p.budzelaar@unina.it.

ORCID

Peter H. M. Budzelaar: 0000-0003-0039-4479

Present Addresses

[‖]R.S.S.: Department of Chemistry, The University of British Columbia, 2036 Main Mall, Vancouver, British ColumbiaV6H 1Z1, Canada.

[⊥]G.S.B.: Exigence Technologies Inc., 200-135 Innovation Drive, Winnipeg, Manitoba R3T 6A8, Canada.

Notes

The authors declare no competing financial interest.

■ ACKNOWLEDGMENTS

This work was supported in part by the National Science and Engineering Council (NSERC RGPIN-04766) and by the Science Foundation of China University of Petroleum, Beijing (No. 2462013YJRC019). We are grateful to Mr. M. Cooper, Dr. F. Hawthorne, and Dr. D. Herbert for help with X-ray diffraction measurements.

■ ABBREVIATIONS

BDI, β-diiminate; COE, cyclooctene

■ REFERENCES

(1) Kawamura, K.; Hartwig, J. F. *J. Am. Chem. Soc.* **2001**, *123*, 8422−8423.

(2) Chen, H. Y.; Schlecht, S.; Semple, T. C.; Hartwig, J. F. *Science* **2000**, *287*, 1995−1997.

(3) Arndtsen, B. A.; Bergman, R. G.; Mobley, T. A.; Peterson, T. H. *Acc. Chem. Res.* **1995**, *28*, 154−162.

(4) Bengali, A. A.; Schultz, R. H.; Moore, C. B.; Bergman, R. G. *J. Am. Chem. Soc.* **1994**, *116*, 9585−9589.

(5) Gilbert, T. M.; Bergman, R. G. *Organometallics* **1983**, *2*, 1458−1460.

(6) Fernandez, M. J.; Bailey, P. M.; Bentz, P. O.; Ricci, J. S.; Koetzle, T. F.; Maitlis, P. M. *J. Am. Chem. Soc.* **1984**, *106*, 5458−5463.

(7) The term "spectroscopic oxidation state" is frequently used. However, there is no reason the oxidation states deduced from several spectroscopic techniques would agree with each other or e.g. with X-ray studies.

(8) Ricci, J. S.; Koetzle, T. F.; Fernandez, M. J.; Maitlis, P. M.; Green, J. C. *J. Organomet. Chem.* **1986**, *299*, 383−389.

(9) Fernandez, M. J.; Maitlis, P. M. *J. Chem. Soc., Dalton Trans.* **1984**, 2063−2066.

(10) Ricci, J. S., Jr.; Koetzle, T. F.; Fernandez, M.; Maitlis, P. M. *Acta Crystallogr., Sect. A: Found. Crystallogr.* **1984**, *40*, C301−C301.

(11) Duckett, S. B.; Haddleton, D. M.; Jackson, S. A.; Perutz, R. N.; Poliakoff, M.; Upmacis, R. K. *Organometallics* **1988**, *7*, 1526−1532.

(12) Duckett, S. B.; Perutz, R. N. *J. Chem. Soc., Chem. Commun.* **1991**, 28−31.

(13) Schubert, U. *Adv. Organomet. Chem.* **1990**, *30*, 151−187.

(14) Scherer, W.; Meixner, P.; Batke, K.; Barquera-Lozada, J. E.; Ruhland, K.; Fischer, A.; Eickerling, G.; Eichele, K. *Angew. Chem., Int. Ed.* **2016**, *55*, 11673−11677.

(15) Vyboishchikov, S. F.; Nikonov, G. I. *Organometallics* **2007**, *26*, 4160−4169.

(16) Taw, F. L.; Bergman, R. G.; Brookhart, M. *Organometallics* **2004**, *23*, 886−890.

(17) Klei, S. R.; Tilley, T. D.; Bergman, R. G. *J. Am. Chem. Soc.* **2000**, *122*, 1816−1817.

(18) Cook, K. S.; Incarvito, C. D.; Webster, C. E.; Fan, Y. B.; Hall, M. B.; Hartwig, J. F. *Angew. Chem., Int. Ed.* **2004**, *43*, 5474−5477.

(19) Hartwig, J. F.; Cook, K. S.; Hapke, M.; Incarvito, C. D.; Fan, Y. B.; Webster, C. E.; Hall, M. B. *J. Am. Chem. Soc.* **2005**, *127*, 2538−2552.

(20) Gilbert, T. M.; Hollander, F. J.; Bergman, R. G. *J. Am. Chem. Soc.* **1985**, *107*, 3508−3516.

(21) Schubert, U.; Kunz, E.; Harkers, B.; Willnecker, J.; Meyer, J. *J. Am. Chem. Soc.* **1989**, *111*, 2572−2574.

(22) Ekkert, O.; White, A. J. P.; Toms, H.; Crimmin, M. R. *Chem. Sci.* **2015**, *6*, 5617−5622.

(23) Budzelaar, P. H. M.; Moonen, N. N. P.; de Gelder, R.; Smits, J. M. M.; Gal, A. W. *Eur. J. Inorg. Chem.* **2000**, *2000*, 753−769.

(24) Budzelaar, P. H. M.; Moonen, N. N. P.; de Gelder, R.; Smits, J. M. M.; Gal, A. W. *Chem. - Eur. J.* **2000**, *6*, 2740−2747.

(25) Bernskoetter, W. H.; Lobkovsky, E.; Chirik, P. J. *Chem. Commun.* **2004**, 764−765.

(26) Zhu, D.; Budzelaar, P. H. M. *Dalton Trans.* **2013**, *42*, 11343−54.

(27) Zhu, D.; Kozera, D. J.; Enns, K. D.; Budzelaar, P. H. M. *Angew. Chem., Int. Ed.* **2012**, *51*, 12211−12214.

(28) Cheng, C.; Hartwig, J. F. *Science* **2014**, *343*, 853−857.

(29) Cheng, C.; Hartwig, J. F. *J. Am. Chem. Soc.* **2015**, *137*, 592−595.

(30) Ghavtadze, N.; Melkonyan, F. S.; Gulevich, A. V.; Huang, C.; Gevorgyan, V. *Nat. Chem.* **2014**, *6*, 122−125.

(31) Meier, G.; Steck, V.; Braun, B.; Eiler, A.; Herrmann, R.; Ahrens, M.; Laubenstein, R.; Braun, T. *Eur. J. Inorg. Chem.* **2014**, *2014*, 2793−2808.

(32) Mcbee, J. L.; Escalada, J.; Tilley, T. D. *J. Am. Chem. Soc.* **2009**, *131*, 12703−12713.

(33) The alternative possibility of fast dissociation for these Ir complexes seems improbable, since according to the DFT results Ir consistently binds its HE ligands more strongly than Rh.

(34) Bagno, A.; Casella, G.; Saielli, G. *J. Chem. Theory Comput.* **2006**, *2*, 37−46.

(35) This change also increases steric hindrance, as the larger CF_3 groups result in increased C−N−C angles.

(36) The addition process can be thought of as a combination of σ-complex formation (donation from HE to M) and true oxidative addition (use of electrons on M to form new M−E and M−H bonds). It would be preferable to have separate scales for these two processes, but we do not see an obvious approach for that.

(37) Crabtree, R. H.; Holt, E. M.; Lavin, M.; Morehouse, S. M. *Inorg. Chem.* **1985**, *24*, 1986−1992.

DOI: 10.1021/acs.organomet.7b00469
Organometallics XXXX, XXX, XXX−XXX

(38) Vincent, J. L.; Luo, S.; Scott, B. L.; Butcher, R.; Unkefer, C. J.; Burns, C. J.; Kubas, G. J.; Lledos, A.; Maseras, F.; Tomas, J. *Organometallics* **2003**, *22*, 5307−5323.
(39) Ekkert, O.; White, A. J. P.; Crimmin, M. R. *Angew. Chem., Int. Ed.* **2016**, *55*, 16031−16034.
(40) Use of Sn_2Me_6 instead of $SnMe_4$ was also explored but did not lead to cleaner chemistry.
(41) Signed average of four coupling constants: ((258 − 49) + (134 − 29))/4 = 79 Hz, assuming the two small values correspond to $^2J_{SnH}$ values.
(42) Hamilton, D. G.; Crabtree, R. H. *J. Am. Chem. Soc.* **1988**, *110*, 4126−4133.
(43) Desrosiers, P. J.; Cai, L. H.; Lin, Z. R.; Richards, R.; Halpern, J. *J. Am. Chem. Soc.* **1991**, *113*, 4173−4184.
(44) Ding, Y. Q.; Hao, H. J.; Roesky, H. W.; Noltemeyer, M.; Schmidt, H. G. *Organometallics* **2001**, *20*, 4806−4811.
(45) Ding, Y. Q.; Ma, Q. J.; Roesky, H. W.; Herbst-Irmer, R.; Uson, I.; Noltemeyer, M.; Schmidt, H. G. *Organometallics* **2002**, *21*, 5216−5220.
(46) Zhu, H. P.; Chai, J. F.; Stasch, A.; Roesky, H. W.; Blunck, T.; Vidovic, D.; Magull, J.; Schmidt, H. G.; Noltemeyer, M. *Eur. J. Inorg. Chem.* **2004**, *2004*, 4046−4051.
(47) Hitchcock, P. B.; Lappert, M. F.; Protchenko, A. V. *Chem. Commun.* **2005**, 951−953.
(48) Basuli, F.; Bailey, B. C.; Huffman, J. C.; Mindiola, D. J. *Organometallics* **2005**, *24*, 3321−3334.
(49) Driess, M.; Yao, S. L.; Brym, M.; van Wullen, C. *Angew. Chem., Int. Ed.* **2006**, *45*, 4349−4352.
(50) Bambirra, S.; Perazzolo, F.; Boot, S. J.; Sciarone, T. J. J.; Meetsma, A.; Hessen, B. *Organometallics* **2008**, *27*, 704−712.
(51) Sarish, S. P.; Nembenna, S.; Roesky, H. W.; Ott, H.; Pal, A.; Stalke, D.; Dutta, S.; Pati, S. K. *Angew. Chem., Int. Ed.* **2009**, *48*, 8740−8742.
(52) Yao, S. L.; Xiong, Y.; Driess, M. *Chem. Commun.* **2009**, 6466−6468.
(53) Adhikari, D.; Basuli, F.; Orlando, J. H.; Gao, X. F.; Huffman, J. C.; Pink, M.; Mindiola, D. J. *Organometallics* **2009**, *28*, 4115−4125.
(54) Uhl, W.; Jana, B. *J. Organomet. Chem.* **2009**, *694*, 1101−1106.
(55) Jana, A.; Roesky, H. W.; Schulzke, C. *Dalton Trans.* **2010**, *39*, 132−138.
(56) Wang, W. Y.; Inoue, S.; Yao, S. L.; Driess, M. *Organometallics* **2011**, *30*, 6490−6494.
(57) Yao, S. L.; Xiong, Y.; Wang, W. Y.; Driess, M. *Chem. - Eur. J.* **2011**, *17*, 4890−4895.
(58) Xiong, Y.; Yao, S. L.; Driess, M. *Chem. - Asian J.* **2012**, *7*, 2145−2150.
(59) Liu, P.; Zhang, Y.; Yao, Y. M.; Shen, Q. *Organometallics* **2012**, *31*, 1017−1024.
(60) Arrowsmith, M.; Hill, M. S.; Kociok-Kohn, G.; MacDougall, D. J.; Mahon, M. F.; Mallov, I. *Inorg. Chem.* **2012**, *51*, 13408−13418.
(61) Abdalla, J. A. B.; Riddlestone, I. M.; Tirfoin, R.; Aldridge, S. *Angew. Chem., Int. Ed.* **2015**, *54*, 5098−5102.
(62) Van der Ent, A.; Onderdelinden, A. L. *Inorg. Synth.* **1990**, *28*, 90.
(63) Cheng, M.; Moore, D. R.; Reczek, J. J.; Chamberlain, B. M.; Lobkovsky, E. B.; Coates, G. W. *J. Am. Chem. Soc.* **2001**, *123*, 8738−8749.
(64) Fulmer, G. R.; Miller, A. J. M.; Sherden, N. H.; Gottlieb, H. E.; Nudelman, A.; Stoltz, B. M.; Bercaw, J. E.; Goldberg, K. I. *Organometallics* **2010**, *29*, 2176−2179.
(65) Budzelaar, P. H. M. *gNMR, 5.0.6*; IvorySoft, 2006; http://home.cc.umanitoba.ca/~budzelaa/gNMR/gNMR.htmlhttp://home.cc.umanitoba.ca/~budzelaa/gNMR/gNMR.html
(66) Sheldrick, G. M. *SADABS*; University of Göttingen, Göttingen, Germany, 1996.
(67) Sheldrick, G. M. *Acta Crystallogr., Sect. A: Found. Crystallogr.* **2008**, *64*, 112−122.
(68) Tao, J. M.; Perdew, J. P.; Staroverov, V. N.; Scuseria, G. E. *Phys. Rev. Lett.* **2003**, *91*, 146401.
(69) Weigend, F.; Furche, F.; Ahlrichs, R. *J. Chem. Phys.* **2003**, *119*, 12753−12762.
(70) *TURBOMOLE, V6.3*; TURBOMOLE GmbH, since 2007: Karlsruhe, Germany, 2011.
(71) Baker, J. *J. Comput. Chem.* **1986**, *7*, 385−395.
(72) Baker, J. *PQS, 2.4*; Parallel Quantum Solutions, Fayetteville, AR, 2001.
(73) Raucoules, R.; de Bruin, T.; Raybaud, P.; Adamo, C. *Organometallics* **2009**, *28*, 5358−5367.
(74) Tobisch, S.; Ziegler, T. *J. Am. Chem. Soc.* **2004**, *126*, 9059−9071.
(75) Grimme, S.; Antony, J.; Ehrlich, S.; Krieg, H. *J. Chem. Phys.* **2010**, *132*, 154104.
(76) Frisch, M. J.; Trucks, G. W.; Schlegel, H. B.; Scuseria, G. E.; Cheeseman, J. R.; Scalmani, G.; Barone, V.; Mennucci, B.; Petersson, G. A.; Nakatsuji, H.; Caricato, M.; Li, X.; Hratchian, H. P.; Izmaylov, A. F.; Bloino, J.; Zheng, G.; Sonnenberg, J. L.; Hada, M.; Ehara, M.; Toyota, K.; Fukuda, R.; Hasegawa, J.; Ishida, M.; Nakajima, T.; Honda, Y.; Kitao, O.; Nakai, H.; Vreven, T.; Montgomery, J. A., Jr.; Peralta, J. E.; Ogliaro, F.; Bearpark, M.; Heyd, J. J.; Brothers, E.; Kudin, K. N.; Staroverov, V. N.; Kobayashi, R.; Normand, J.; Raghavachari, K.; Rendell, A.; Burant, J. C.; Iyengar, S. S.; Tomasi, J.; Cossi, M.; Rega, N.; Millam, J. M.; Klene, M.; Knox, J. E.; Cross, J. B.; Bakken, V.; Adamo, C.; Jaramillo, J.; Gomperts, R.; Stratmann, R. E.; Yazyev, O.; Austin, A. J.; Cammi, R.; Pomelli, C.; Ochterski, J. W.; Martin, R. L.; Morokuma, K.; Zakrzewski, V. G.; Voth, G. A.; Salvador, P.; Dannenberg, J. J.; Dapprich, S.; Daniels, A. D.; Farkas, O.; Foresman, J. B.; Ortiz, J. V.; Ciolowski, J.; Fox, D. J. *Gaussian 09, B.01*; Gaussian, Inc., Wallingford, CT, 2009.
(77) Hay, P. J.; Wadt, W. R. *J. Chem. Phys.* **1985**, *82*, 299−310.
(78) Hay, P. J.; Wadt, W. R. *J. Chem. Phys.* **1985**, *82*, 270−283.
(79) Wadt, W. R.; Hay, P. J. *J. Chem. Phys.* **1985**, *82*, 284−298.

DOI: 10.1021/acs.organomet.7b00469
Organometallics XXXX, XXX, XXX−XXX